Tutors
Cristina Balcells
Dr. Francesc Mas
Departament de Química Física

Grau de Química

Treball Final de Grau

Effect of macromolecular crowding on the kinetics of enzymatic reactions catalysed by oligoproteins. The LDH dimer-tetramer case.

Efecte del *crowding* macromolecular en la cinètica de reaccions enzimàtiques catalitzades per oligoproteïnes. El cas del dímer-tetràmer de la LDH.

Núria Vilaplana Lopera

June 2015

Universitat de Barcelona

B:KC Barcelona Knowledge Campus

La motivació d'un científic és principalment la curiositat i el desig de la veritat.

Irving Langmuir

M'agradaria agrair el seu ajut, consell i suport:

Al Dr. Francesc Mas, per introduir-me al món del *crowding* i de la cinètica enzimàtica de forma pacient i motivadora, traient-me la por a les equacions i els models i creient en mi.

A la Cristina Balcells, per la seva increïble paciència, el seu inestimable ajut, per les estones genials que hem passat treballant juntes i per haver-me acollit tan amablement. Gràcies per transmetre'm la teva passió i per canviar-me per complet la forma de veure el món de la bioquímicafísica.

A la Claudia Hernández, per tot el suport i ajut, per fer el treball molt més divertit i per animar-me en els pitjors moments de la forma més amable i sincera.

A la meva família, pel seu suport incondicional i perquè sense ells no hauria arribat a on estic.

Al Carlo, per recolzar-me sempre, motivant-me i animant-me, i per fer petits tots els problemes.

Gràcies de tot cor.

REPORT

CONTENTS

1. SUMMARY

A study on the enzyme kinetics of L-lactate dehydrogenase, which catalyses the reduction of pyruvate to lactate oxidizing NADH, is presented. This reaction occurs when a lack of oxygen is present and is related to muscular fatigue. LDH is one of the most important biomarkers of injuries and disease, because it is released during tissue breakdown.

General concepts of enzyme kinetics have been reviewed and some models to explain the kinetics of the enzyme have been proposed. L-lactate dehydrogenase is a tetrameric protein, an enzyme formed by four subunits, and the presence of a possible cooperativity, i.e., different affinity in each active centre, must be considered. Besides, macromolecular crowding, the alteration of the behaviour of molecules with the presence of highly concentrated macromolecules, and its possible effects on enzyme kinetics have been presented.

A series of experiments, measuring the initial velocity of the reaction by spectrophotometric means and using a stopped-flow methodology, have been performed. The experiments have been carried out varying the pyruvate and the enzyme concentration and working in solution conditions. A series of experiments in crowded media, at high macromolecules concentration, have been performed. The crowded media experiments have been carried out using different obstacle sizes, using dextran polymer to simulate the cellular crowding, and with different enzyme concentrations.

A surface plot of initial velocity as a function of substrate and enzyme concentrations, for the solution media data, has been obtained. The data has been fitted to the proposed models and the results have suggested an ideal behaviour without cooperativity. In crowded media, a higher decrease in the reaction velocity has been found when using the bigger dextran and the higher enzyme concentration. An auto-crowding hypothesis, the enzyme acts itself as a crowding agent, is presented to possibly explain the results.

Keywords: Enzyme kinetics, Macromolecular crowding, Cooperativity, L-lactate dehydrogenase.

2. RESUM

S'ha realitzat un estudi sobre la cinètica enzimàtica que presenta la L-lactat deshidrogenasa quan catalitza la reducció de transformació de piruvat a lactat mitjançant l'oxidació de NADH. Aquesta reacció es dóna quan hi ha un dèficit d'oxigen i està relacionada amb la fatiga muscular. La LDH és un dels biomarcadors més importants ja que permet identificar malalties i lesions perquè s'allibera durant el trencament de teixits.

S'han revisat els principals conceptes de cinètica enzimàtica i s'han proposat uns models per explicar el comportament cinètic de l'enzim. La L-lactat deshidrogenasa és un tetràmer, un enzim format per quatre subunitats, i s'ha estudiat la possibilitat de que presenti un comportament cooperatiu, i.e., diferent afinitat en cada centre actiu. També s'ha introduït el concepte del *crowding* macromolecular: la alteració del comportament de les molècules en presència de macromolècules altament concentrades; i els seus possibles efectes en la cinètica enzimàtica.

S'han dut a terme un seguit d'experiments en els quals s'ha obtingut la velocitat de reacció mitjançant mesures espectrofotomètriques amb un sistema de Stopped-Flow. Aquests experiments s'han realitzat variant les concentracions de piruvat i d'enzim, treballant en dissolució. També s'han realitzat experiments en medi *crowding*: amb una alta concentració de macromolècules; utilitzant mides diferents dextrans, que són els agents que simularan el *crowding* cel·lular, i amb concentracions diferents d'enzim.

S'ha obtingut un gràfic de superfície de la velocitat inicial en funció de les concentracions d'enzim i de substrat, per les dades en dissolució, i s'han ajustat les dades als models proposats. Els resultats suggereixen un comportament ideal sense cooperativitat. Pel que fa als experiments en medi *crowding*, s'ha obtingut un descens en la velocitat de reacció més gran amb el dextrà de major mida amb l'enzim més concentrat. S'ha proposat una hipòtesi per explicar els resultats: l'*auto-crowding*, en el qual el propi enzim actua com a *crowder*.

Paraules clau: Cinètica enzimàtica, *Crowding* macromolecular, Cooperativitat, L-lactat deshidrogenasa.

3. INTRODUCTION

The enzyme that we are going to study is L-lactate dehydrogenase (LDH). A dehydrogenase is an enzyme that transfers hydrides. L-lactate dehydrogenase catalyses the reaction to convert pyruvate into lactate by oxidizing NADH into NAD^+, as we can see at Scheme 1. When a tissue is injured, LDH is released into the bloodstream[1] and this effect can be used as biomarker of tissue breakdown. LDH converts pyruvate to lactate when there is a lack of oxygen and catalyses the reverse reaction during the Cori cycle in the liver[1]. L-lactate dehydrogenase has been related to muscular fatigue[2], which is caused by the accumulation of lactic acid during intense exercise periods.

The reaction can be followed by spectrophotometric measurements due to a change in its absorbance when NADH, which absorbs at 340 nm, is converted in NAD^+, which no longer absorbs at 340 nm. [3]

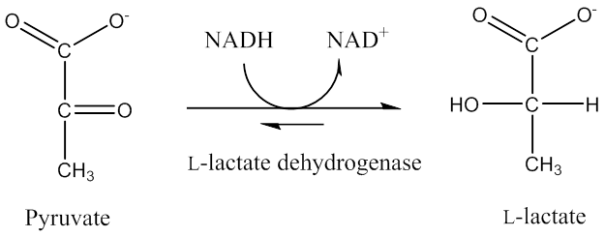

Scheme 1. The reaction of pyruvate with NADH catalysed by L-lactate dehydrogenase.

L-lactate dehydrogenase is known to be oligomeric[4]: it is formed by more than one subunit of protein. Oligoproteins are formed by different subunits connected by non-covalent bonds: monomers, dimers, tetramers... LDH can be a homo or hetero tetramer composed by all possible combinations of M (muscle) or H (heart) subunits. The LDH isoenzyme that has been used in our experiments is formed by four M subunits and this kind of LDH is found in the liver and in the muscles. [4]

It is usually considered that all the catalytic centres in oligomeric proteins have the same activity and that they follow the Michaelis-Menten model. But some of them present

cooperativity; they have different enzymatic activity depending on the number of substrates united. Cooperativity influences the effect of these proteins in cell metabolism.

Enzyme kinetics data have been usually obtained working in dilute solutions but, inside the living cell, we find high concentrations of macromolecules of different sizes and shapes up to 40% of the volume[5] of cytosol. This means that almost all the biochemical data do not reflect the *in vivo* conditions. Certainly, performing the experiments in *in vivo* media would be the best solution but obtaining reproducible data without interferences of other species would be difficult and even more if the reaction is fast, as in the present case. Besides, in our case, NADH is a coenzyme that is used in a lot of biochemical reactions at a time and its fluctuation in the cell depends on a high number of variables and different reactions. It would be nearly impossible to follow the change in the absorbance caused by NADH of this reaction in *in vivo* media.

To facilitate the understanding of enzyme kinetics and to obtain plausible values of the kinetic parameters, studies that simulate the macromolecular crowding in the cell were proposed[6-13]. Macromolecular crowding studies the modification of diffusive processes, reactions and interactions inside the cell, due to high concentrations of neighbouring macromolecules present in the intracellular medium[14]. It is important to study biochemical processes in nature-like environments, trying to recreate the effect of such concentrations; to obtain accurate rates for enzymatic reactions.

The aim of performing experiments in crowded media is to find a middle ground between performing experiments in *in vivo* or *in vitro* media. This is supposed to renew the kinetic databases because as said previously: until recently, all the enzyme kinetics experiments were performed in diluted solution media. It can also be useful, for example, to drug design or systems biology.

As an introduction, we are going to briefly summarize some related enzyme kinetics theories and equations and some important aspects of macromolecular crowding on enzyme kinetics.

The aim of this work is the study of the kinetics of L-lactate dehydrogenase, varying systematically the enzyme concentration. Furthermore, variations in the kinetic parameters as experimental conditions change, when a crowding agent is added, will be interpreted. We are going to compare the variation of these parameters when we work in dilute solution and when we add increasing amounts of excluded volume, provided by dextran polymers. We will try to find out if there is some type of cooperativity in our enzyme, we will try to fit the experimental

data to a novel model based on the Michaelis-Menten theory and the steady-state assumption and we will compare the value of some kinetic parameters when working in solution and when working under crowding conditions.

3.1. ENZYME KINETICS

Enzymes are proteins that catalyse biological reactions; they increase the rate of these reactions by making them kinetically favourable. Enzymatic catalysis is essential for living systems: metabolic processes need enzymes and it is indispensable to know its operation and how they affect the kinetics of the reactions they catalyse.

In the present section we are going to review a general kinetic model that will be useful to explain the behaviour of our enzyme, L-lactate dehydrogenase.

3.1.1. The Michaelis-Menten equation

Leonor Michaelis and Maud Menten in 1913[15, 16] postulated a model to explain the kinetics of most of the enzyme catalysed reactions. The Michaelis-Menten equation relates the initial velocity with the substrate concentration and it is usually expressed like:

$$v_0 = \frac{v_{max}+[S]}{K_m+[S]} \qquad \text{(Eq. 1)}$$

The model is based on this scheme:

$$E + S \underset{k_{-1}}{\overset{k_1}{\rightleftharpoons}} ES \xrightarrow{k_2} E + P$$

Scheme 2. Representation of a Michaelis-Menten enzymatic reaction. The enzyme (E) reacts with the substrate (S) to form a reversible complex (ES) that decomposes into the enzyme and the product (P).

The enzyme (E) is first combined with the substrate (S) forming a reversible complex (ES) in a fast step. The complex is decomposed in a slower second step to form the product (P) and liberate the enzyme. The constant k_2 is also called catalytic constant, $k_{cat,}$ or turnover number.

To deduce the Michaelis-Menten expression (Eq. 1) we must make several assumptions. First, we are measuring initial rates, our system is under initial conditions and it can be assumed that the reaction of the decomposition of the complex to form the product is irreversible; no equilibrium is established in the decomposition reaction.

Another benefit of measuring initial rates is that, provided that the substrate concentration is much higher than enzyme concentration, we can consider that the enzyme is saturated. Usually initial substrate concentration is five or six orders of magnitude greater than enzyme concentration so if we only measure initial rates the variation in substrate concentration can be neglected and we can consider that it remains constant.

Now we need to define the rate equation, which will be expressed as the rate of product formation, described as:

$$v = \frac{d[P]}{dt} = k_2[ES] \quad \text{(Eq. 2)}$$

The problem that appears is that it is difficult to know the complexed enzyme concentration, as well as knowing the free enzyme concentration at a given time of the reaction, so we need to find a new species of which we know its exact concentration throughout the reaction.

The enzyme exists in its free form and in its complex form all over the reaction. In lower substrate concentrations, enzyme will be in its free form majorly and it will be forced to form the complex. However, in higher substrate concentrations, a significant part of the enzyme will be in its complex form and an increase in substrate concentration will have no effect on rate: we will be on the *plateau* of the reaction.

If we write the mass balance for the enzyme:

$$[E]_t = [E] + [ES] \quad \text{(Eq. 3)}$$

We can now relate the complex concentration to the enzyme total concentration ($[E]_t$) which is the enzyme concentration on the reacting mixture initially, and therefore its exact concentration is known. Now we need to express the rate equation in terms of $[E]_t$, and substrate concentration, $[S]$, which will be the magnitude with a measurable variation.

Next, we need to make the assumption that the complex intermediate concentration reaches a stationary regime: its concentration remains constant. Otherwise, Equation 4, which is the kinetic rate law considering Scheme 2, would not be analytically resoluble.

$$0 = \frac{d[ES]}{dt} = k_1[E][S] - k_2[ES] - k_{-1}[ES] \quad \text{(Eq. 4)}$$

Equalling Equation 4 to zero, which is known as the steady-state approximation, and rearranging terms we obtain:

$$k_1[E][S] = (k_2 + k_{-1})[ES] \quad \text{(Eq. 5)}$$

This leads us to the next expression, which is known as the Michaelis constant.

$$\frac{[E][S]}{[ES]} = \frac{k_2 + k_{-1}}{k_1} \equiv K_m \quad \text{(Eq. 6)}$$

This constant is equivalent to the equilibrium constant of the decomposition of the complex in substrate and free enzyme.

If we isolate the free enzyme concentration and substitute it in the enzyme mass balance, we will have an expression for the complex concentration in terms of $[E]_t$ and $[S]$.

$$[E]_t = \frac{K_m[ES]}{[S]} + [ES] \rightarrow [ES] = \frac{[E]_t[S]}{K_m + [S]} \quad \text{(Eq. 7)}$$

As stated before, E concentration is known only initially, when all the enzyme is in its free form, and S concentration, by means of substrate depletion or product formation, can be monitored during the course of the reaction by a wide range of experimental techniques.

Finally, if we substitute the equation for $[ES]$ in the rate equation we get:

$$v = \frac{k_2[E]_t[S]}{K_m + [S]} \quad \text{(Eq. 8)}$$

Now, the only difference between Equation 1 and Equation 8 is v_{max}. To introduce the maximum velocity term (v_{max}), we need to think that the rate of the reaction at a given instant *t* will be given by the expression $v = k_2[ES]$. Therefore, the maximum velocity that the reaction could hypothetically achieve would occur when $[ES]$ value reaches its maximum, which cannot be higher than $[E]_t$. This cannot be achieved experimentally in a real situation, but rather represents an asymptotic value as $[S]$ approaches an infinite value.

$$v_{max} = \lim_{[S]\rightarrow\infty} v = k_2[E]_t \quad \text{(Eq. 9)}$$

Now the rate equation can be expressed as:

$$v = \frac{v_{max}[S]}{K_m + [S]} \quad \text{(Eq. 1)}$$

This is the most usual form of the Michaelis-Menten equation. This expression can be represented as:

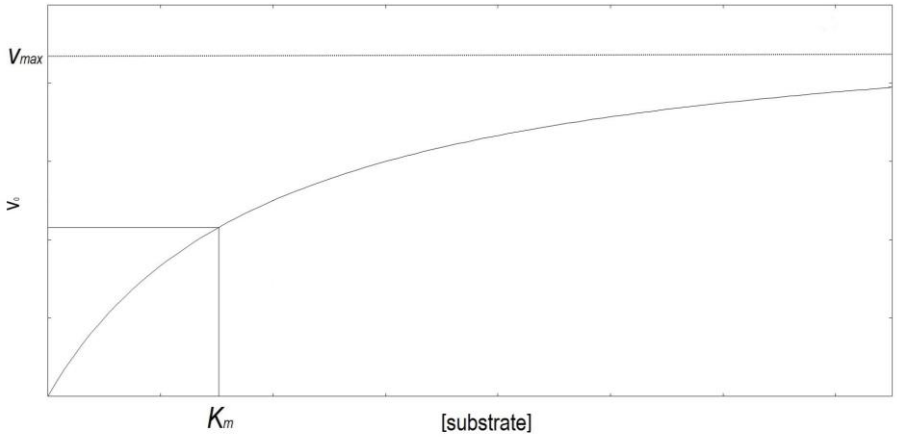

Figure 1. The variation of initial rate with substrate concentration following a Michaelis-Menten curve (hyperbola).

In Figure 1 we can see how initial rate varies with substrate concentration in a typical enzyme reaction. In lower substrate concentrations, initial rate increases linearly with substrate concentration. In higher substrate concentrations, initial rate increases more and more slowly until it reaches a plateau; this plateau is the maximum rate, v_{max}. The shape of this curve is a hyperbola with an asymptote which has the value of v_{max}.

In the experimental data analysis we will represent the initial rate against substrate concentration and, if the curve is of a Michaelis-Menten type, we will fit it to this equation. Once is fitted, we will find v_{max} and K_m and this values we will used to be compared with the ones obtained with different enzyme concentrations.

3.2. MACROMOLECULAR CROWDING

As defined previously, the macromolecular crowding phenomenon is based on some alterations of the physicochemical properties of macromolecules due to the existence of high concentrations of unrelated macromolecules in the solution. This effect usually appears in cellular environments where biopolymers present in the cell cytosol act as crowders reducing the volume of solvent available, which increases the effective concentration of all the species involved in a reaction process. [14]

We say that the media is crowded rather than concentrated because in cellular environments there is not a high concentration of a single macromolecule but a lot of different macromolecules that taken together occupy between 5% and 40%[5] of the total volume in the cell. If we compare the macromolecular concentration in crowded media, 50-400 mg/mL, against in vitro conditions, 1-10 mg/mL, we will see that performing enzymatic experiments in vitro is not representing real cellular conditions at all[5]. Thus, all processes that take place in the cell are quite afar from ideality.

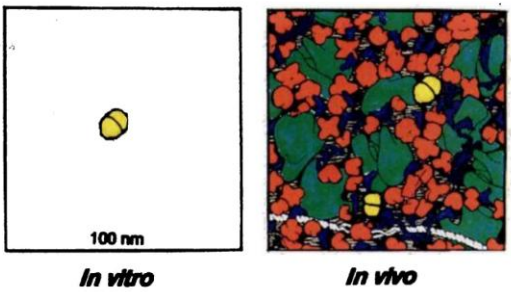

Figure 2. The difference between *in vivo* and *in vitro* systems.
(Extracted image from Ellis & Hartl. *FASEBJ* . **1996** 10: 20-26.)

The number of published studies of macromolecular interactions has increased in the past years. However, most of them are aimed at the characterization of attractive interactions that result in the formation of protein complexes or protein and other macromolecules complexes. Repulsive interactions may not be observed directly because they do not form complexes. The presence and significance of these interactions in crowded media may be observed indirectly through their effects on a variety of macromolecular reactions.

Most of the effects produced by repulsive interactions may be predicted qualitatively, and sometimes quantitatively, using simple statistical-thermodynamic models and observed

experimentally. To this end we can measure the dependence of thermodynamic solution properties and reaction kinetics and equilibria on the concentration and composition of the crowders, macromolecular cosolutes that are nominally inert with respect to the reaction of interest. [17]

The excluded volume of a molecule is the volume that is inaccessible to other molecules in the system as a result of the presence of the first molecule[18]. We can see how the excluded volume of macromolecular crowders can affect our reaction in Figure 3. The excluded volume interactions are important because they are universal and nonspecific and they have the potential to significantly modulate the kinetics and equilibria of a large number of macromolecular reactions that take place in physiological fluid media.

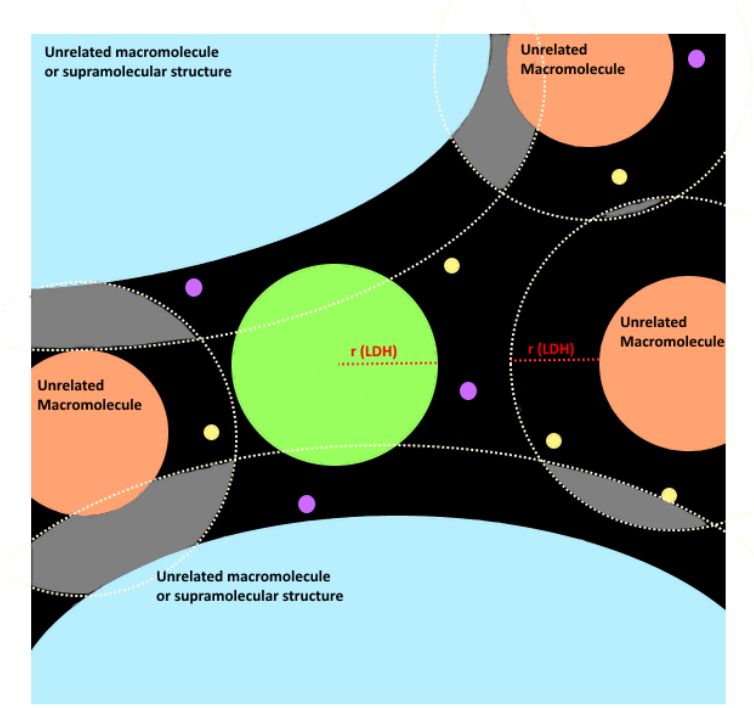

Figure 3. An schematic representation of the excluded volume phenomenon in our reaction. The green round is our enzyme, the blue rounds are unrelated macromolecules or supramolecular structures, orange rounds are unrelated macromolecules, yellow and purple rounds are substrates and the indicated radius is the excluded volume, the paths were the enzyme cannot pass.

Another volume exclusion phenomenon present in the cell and related to macromolecular crowding is macromolecular confinement. It is defined as the conjunct of effects of excluded volume on the free energy and reactivity of a macromolecule situated in a cavity bounded by impenetrable walls having a smallest interior dimension only slightly larger than the largest dimension of the macromolecule. [17]

The difference between macromolecular crowding and confinement is that macromolecular crowding is referred to the volume exclusion effect of one soluble macromolecule to another and macromolecular confinement is attributed to the volume exclusion effect of a fixed boundary to a soluble macromolecule.

3.2.1. General aspects of macromolecular crowding

Macromolecular crowding can affect in a unique manner on some variables contributing to the enzymatic rate such as: diffusion, binding, thermodynamic activity and enzyme stability.

Under the effect of excluded volume, macromolecules tend to rearrange themselves to their most compact conformation, so as to minimize steric repulsions. Then if we consider an enzyme with multiple conformations, excluded volume will shift the equilibrium toward the most compact conformation. In this regard, macromolecular crowding enhances the stability of enzymes by favouring they folded conformation. Equally, if an enzyme presents an equilibrium between individual monomers and a more compact dimer, crowding will favour the dimer. [17, 19]

Crowding can change the value of Michaelis constant (K_m) as well as the k_2 value. The k_2 value, as well as the v_{max} value, is expected to decrease in crowded media because crowding usually hinders diffusion and difficult enzyme and substrates encounters[11, 13]. The K_m change cannot be predicted.

The nature of the macromolecule used to simulate the crowding effect often affects the results. A protein crowding agent can increase the activity of some enzyme whereas a synthetic crowding polymer, such as dextran, can decrease the enzymatic activity of the same enzyme. Crowding by synthetic polymers promotes protein folding, self-association and binding by stabilizing the enzyme. [12]

Macromolecular crowding is expected to affect diffusion and transport phenomena, decreasing the diffusion coefficient and hindering transport[6]. Crowding also enhances protein stability and favours folded conformations. [19]

3.2.2. Effects of macromolecular crowding on some prototypical reactions

We are going to summarize some experimental effects of macromolecular crowding on some prototypical macromolecular reactions such as bimolecular association, association of a soluble macromolecule ligand with a specific surface binding site and two-state protein folding.

3.2.2.1. Bimolecular association

Bimolecular association reaction can be described as:

$$A + B \rightleftharpoons AB$$

Scheme 3. Representation of the bimolecular association of A and B to form the complex AB.

About equilibria, crowding can substantially enhance the dimerization of A and B when AB is compact but it can also inhibit the tendency of A and B to dimerize when the dimer obtained is so spherical that it excludes more volume to crowder than the two monomers.

The effect of crowding on the equilibrium constant for the association of some monomers increases dramatically as the number of monomers that takes part increases. [17]

In the reaction or transition state control, the rate constant is determined by the energy barrier resulting from the conformational changes that are necessary to form the product. As the transition state for association is generally nearly as compact as the product complex, crowding is expected to lower this energy barrier and increase the association rate. A small effect on the dissociation constant is expected. [20]

Because fast associations are typically under diffusion control and slow associations are under reaction control, crowding is expected to decelerate fast associations and accelerate slow associations.

3.2.2.2. Site-binding

The association of a soluble macromolecular ligand with a specific surface binding site can be described as:

$$L + S \rightleftharpoons LS$$

Scheme 4. Representation of the site-binding of a ligand, L, to a site, S.

Crowding affects only the free ligand because the bounded ligand is buried and inaccessible to crowders.

Theoretical calculations[17] demonstrate that the enhancement of association by crowding can be much more significant for site-binding than for bimolecular associations.

3.2.2.3. Two-state protein folding

The two-state folding of a protein can be represented as:

$$U \rightleftharpoons N$$

Scheme 5. Representation of the folding of a protein: U is the unfolded form and N is the native form (folded).

The presence of crowder influences this equilibrium between conformational states by favouring the conformations that exclude less volume to the crowder.

In this case, with proteins, the unfolded conformations exclude more volume to the crowder because they are more expanded than the folded ones. Therefore, crowding is expected to enhance the presence of the native state. [17]

When the transition state is less compact than the reactant state, crowding is expected to decrease the rate constant.

3.2.3. Previous enzyme kinetics in macromolecular crowding media experiments

3.2.3.1. L-lactate dehydrogenase

A study on the effect of macromolecular crowding on the oxidation of NADH by pyruvate catalysed by L-lactate dehydrogenase[8], the same enzyme that we are studying, found that the reaction rate of the reaction is determined by both the occupied volume and the relative size of the obstacles.

The reaction rate decreased as dextran size increase when it was at high concentrations (100 mg·mL^{-1}). It means that the reaction depends not only on the occupied volume but also on the dimension of the obstacles present in the reaction media. This behaviour can be related to the effect of the relative size of the enzyme respect to the size of the crowder. Only high concentrations of large dextrans affected v_{max} and K_m while smaller sizes of dextrans had a lower decreasing effect.

The reduction in v_{max} can be explained by a decrease of k_{cat} (k_2) as a result of changes in the conformation of the catalytic centre due to the crowded media. But in this case, the catalytic centre is protected from the bulk solution. The other reasonable explaining is that the encounter

between enzymes and substrates is reduced by large dextrans because they have similar size to LDH. And for small dextrans, the decrease in v_{max} is inferior because the crowding effect is partially compensated by an enhancing of the enzymatic activity by a cage effect that is, as defined previously, macromolecular confinement.

The effective diffusion coefficient is lower in crowded media than in dilute solution, and a decrease in this coefficient may decrease k_1. K_m value should increase because of the decrease in k_1, but it remains constant until high concentration of large dextrans. The decrease in K_m with high concentrations of large dextrans can be attributed to a modification on the chemical activity of the substrate due to the non-ideal conditions in crowded media and also by an increase of the activity coefficients relation between the free enzyme and the complex. Besides, the water activity can also affect because the substrate and the active site must be dehydrated for the process of binding, then k_2 must be affected.

3.2.3.2. Other enzymes

A study about the crowding effect on the reaction initial velocity of the hydrolysis of N-succinyl-L-phenyl-Ala-*p*-nitroanilide catalysed by alpha-chymotrypsin[7] showed that the volume occupied by the dextran (equivalent to its concentration) but not its size had a great effect on the initial rate of this reaction. v_{max} decreased and K_m increased with increasing dextran concentrations. The rise in K_m could be explained by a slower diffusion of the enzyme because of the crowding presence. The decrease in v_{max} could be attributed to the effect of mixed inhibition by the product, which is enhanced in crowded media.

Another studied enzyme: horseradish peroxidase[9] (HRP), which catalyses the oxidation of 2,2'-azino-bis(3-ethylbenzothiazoline-6-sulfonate) by hydrogen peroxide, showed an influence by the crowding agent concentration (excluded volume) but not its size. The enzyme kinetics parameters v_{max} and K_m both decreased with an increasing obstacle concentration. It suggested an activation control of the enzymatic reaction, which means that the catalytic constant, k_{cat} (equivalent to k_2), is affected by the crowding environment and has a significant contribution in K_m. The contribution could be explained by an increase in the ratio of activity coefficients of the nature enzyme and the complex due to the presence of crowders, an increase in chemical activity of water because of crowding, a conformational change in the active site of the enzyme induced by crowding or a combination of some of these factors.

A study on malate dehydrogenase[12], which catalyses the oxidation of malate to oxaloacetate reducing NAD^+ to NADH, was performed. One the many experiments that were carried out in that study, showed that the kinetics parameters depend on the size and amount of dextran. In general, any size of dextran decreased the value of v_{max} but dextrans with similar size to MDH size. The K_m values also decreased with any size of dextran but they showed no clear tendency with the dextran sizes.

The hydrolysis of *p*-nitrophenyl phosphate catalysed by alkaline phosphatase[10] (ALKP) was studied and it presented similar behaviour to the reported study of LDH. The reaction rate depended on the excluded volume and the crowder size. The reaction rate showed a pronounced decrease with an increase of excluded volume with larger dextrans. For smaller dextrans the reduction on the initial rate was moderate. This is in concordance with the reported LDH results: larger dextrans reduce the frequency of the enzyme-substrate encounters.

It is necessary to note that ALKP and MDH are active as dimers[10,12], alpha-chymotrypsin and HRP are monomers[7,9] and LDH is a tetramer. [4]

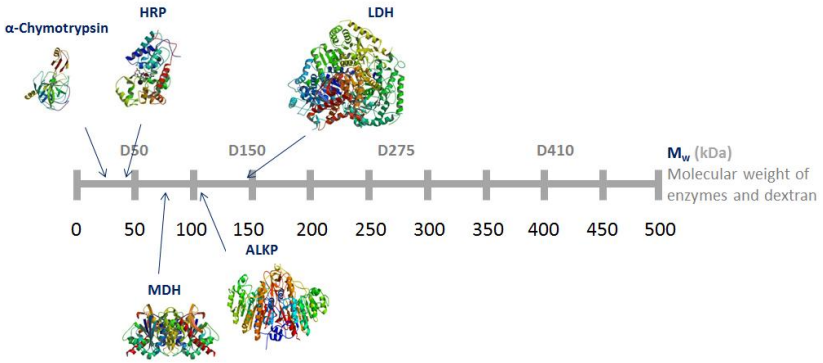

Figure 4. A size scheme including the size of the enzymes reviewed and the dextrans sizes.
(Extracted image from Pastor. et al.. *Biophysical Chemistry*. **2014** *185*: 8–13)

Considering the size of the enzymes, which can be seen in Figure 4, it has been found that small enzymes, like HRP and alpha-chymotrypsin, depend only on the excluded volume of the solution, in other words: of the dextran concentration but not its size. Large enzymes present dependence on the excluded volume and the dextran size. This behaviour can be interpreted as follows: the smaller enzymes are affected only by the excluded volume because they are

smaller than the crowders used and they see them as cell walls; larger enzymes, in contrast, have similar sizes to the crowder sizes and see them as obstacles that diminish its diffusion, reducing the encounters between enzymes and substrates. [11]

In addition to this interpretation, with small obstacles the excluded volume effect is partially offset by a caging effect (related to macromolecular confinement) that enhances the enzyme activity, resulting in a minor decrease of the initial velocity of the reaction.

Other effect that has been appearing is that, for large oligomeric enzymes, the effect of dextrans with similar size is higher than with the other dextran sizes. This effect has been seen on MDH[12] or ALKP[10]. However, the origin of the difference between the effect of obstacle size on this two enzymes and on LDH is not clear yet.

3.2.3.3. Alternative methods

Crowding effects on enzyme kinetics can also be studied by computational simulations. Diffusion-controlled and mixed activation-diffusion reactions in crowded media can be studied performing either Monte Carlo simulations in a three dimensional lattice[21, 22], or Brownian Dynamics simulation for the diffusion process coupled to Monte Carlo simulation for the reaction process, in an off-lattice scheme. [23]

For example, a study on the effect of the enzyme-obstacle relative size revealed that the rate coefficient depends on time for diffusion-controlled bimolecular reactions in crowded media, which is known as a fractal kinetics[24]. And that, in mixed activation-diffusion reactions, the fractality of the reaction decreases as the activation control increases. [22]

Another technique is fluorescence recovery after photobleaching (FRAP) which is a common technique to study diffusion processes of macromolecules. A study on the diffusion of alpha-chymotrypsin[6] in crowded media was performed using a confocal laser scanning microscope. Their results showed that the enzyme present anomalous diffusion depending on the size and concentration of dextrans, until a high concentration of large dextrans is reached. When large dextrans are in high concentrations other phenomena such as microviscosity, hydrodynamics interactions or interplay between branches of dextran should be considered.

Both of these techniques were used in parallel to study diffusion in crowding media and agreed in their results. They both found that enzyme diffusion in alpha-chymotrypsin and in Monte Carlo simulation experiments, presented an anomalous diffusion in crowded media. [25]

4. OBJECTIVES

The aim of this work is to study the enzyme kinetics of the oxidation of NADH by pyruvate, catalysed by L-lactate dehydrogenase (LDH). We want to characterize the kinetics of the reaction and find if the enzyme, LDH, presents any type of cooperativity or not and which model follows. The initial hypothesis of cooperativity arises from a work by Saito, M.[26]. Firstly, different models of cooperativity have been developed, taking into account the possibility of a dimer-tetramer equilibrium. We also want to perform some experiments in crowded media, in order to analyse the effect of crowding on v_{max} and K_m.

All the experiments will consist on measuring the variation of initial rate of the reaction in different concentrations of substrate by spectrophotometric measures of the NADH absorbance during the first seconds. Then, we will estimate the best model that fits the plots of the initial rates against substrate concentration in order to elucidate the best mechanism to explain the experimental results.

First, we will measure in *in vitro* conditions, all solutions will be diluted in pH=7.5 buffer with adjusted ionic strength, and changing systematically enzyme and substrate concentrations. We want to obtain a 3D surface graph with initial rate, substrate concentration and enzyme concentration on the axis. From the surface and other plots related we can fit our data to the models that we have proposed and see which one of them fits the data better. Once we find a model that fits our data properly, we will try to explain the behaviour of our enzyme.

Finally, we will measure in crowded conditions, in comparable conditions to diluted solution. We will prepare our solutions with two different enzyme concentrations, the same substrate concentrations that in dilute solution experiments and adding a certain concentration of dextrans of two determined sizes, one similar to the enzyme and one significantly larger than the enzyme. We will compare the data obtained with the data from the previous experiment to have a comparative plot of solution against dextrans and see how the dextran affects the kinetic parameters

5. EXPERIMENTAL SECTION

5.1. MATERIALS AND METHODS

5.1.1. Reaction

The reaction that we are going to study is the oxidation of NADH by pyruvate, catalysed by L-lactate dehydrogenase (LDH). This reaction was chosen by some reasons: first, it is a well-known reaction; second, there is an absorbance change in the course of the reaction so it can be followed by UV-spectroscopy; third, there is no significant variation in the excluded volume because substrates and products are small; fourth, the enzyme and the type of macromolecular crowder that we are using, dextrans, do not interact; and fifth, the enzyme size is intermediate between the available dextrans.

Due to these many reasons, we can interpret the kinetic parameters to study cooperativity and the effect of macromolecular crowding on this reaction only in terms of the crowding agent presence.

5.1.2. Macromolecular Crowder

In this study we need to simulate cellular conditions and it is reasonable to think of using cell extracts. Nevertheless, obtaining reproducible data without interferences of other species would be very difficult because of the complex media, heterogeneity in geometrical and physical properties of the cell environment. In our case, using a spectrophotometer, it would be nearly impossible to measure only NADH absorbance because a lot of other species absorb and interfere. And besides, NADH depletion could not be accounted only to LDH activity using cell extracts, but also to a great number of other dehydrogenases present in the media.

Instead of that, we are going to use dextrans as crowding agents. There are other substances that can be used on our purpose such as polyethylene glycol, polyvinyl alcohol, Ficolls, ovalbumin, serum album and haemoglobin. We have chosen dextrans due to their

optimal properties and their widespread use in similar studies which will allow us to compare our results.

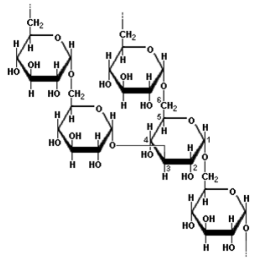

Figure 5. The chemical structure of dextran polymer.

Dextrans are purified macromolecules with no reactivity and highly soluble in water. Its flexibility and random coil shape in solution makes them suitable for modelling many macromolecules present in the natural state of the cell. They are also available in many different sizes and in large quantities.

5.1.3. Stopped-Flow

The Stopped-Flow method is the most widely used method for studying fast reactions. It is essentially composed by: two drive syringes that contain the reacting species, a mixing device, an observation cell, a stopping syringe and a detecting and recording system that can detect changes in a measurable magnitude in a fast way and in small increments of time. [16]

The reaction starts when we push the plungers of the two drive syringes simultaneously. The reactants mix, and the mixture is forced through the observation cell. When we push again the mixture that is in the observation cell is forced into the stopping syringe. A short movement of the plunger of the stopping syringe brings it to a mechanical stop, which prevents further mixing.

The time between the first mixing of reactants and the arrival of the mixture in the observation cell is of the order of 1 ms, and it is called dead time.

In its usual form, the stopped-flow method requires a spectrophotometer for following the course of reaction. This makes it useful for reactions that have large changes of absorbance at a convenient wavelength, such as our case: the oxidation of NADH by pyruvate. However, the

method is not restricted to such cases. It can include and pH indicator, a fluorescence detector, etc.

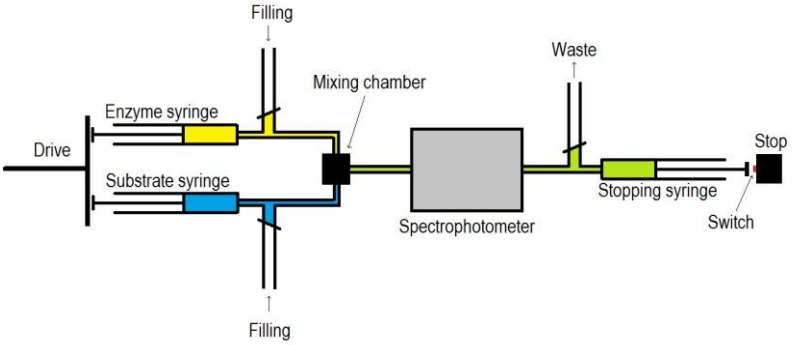

Figure 6. A scheme from the stopped-flow system used.

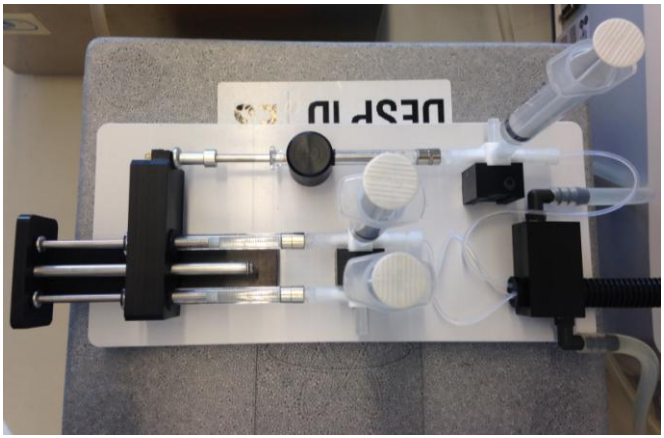

Figure 7. The stopped-flow system used.

In our case we will place a solution with twice the final concentration on cuvette of pyruvate and another solution with twice the concentration of the enzyme plus NADH. The mixing chamber and the measuring cell are thermostatted at 25ºC.

All the system is cleaned with water and ethanol. The samples are injected from less concentrated to the most concentrated in order to minimize error.

5.1.4. Chemicals

Rabbit muscle L-lactate dehydrogenase (E.C.; 140 U mg^{-1}), was received as a purified and lyophilized powder. The enzyme, imidazole (for buffer solution) sodium pyruvate, and β-nicotinamide adenine dinucleotide, reduced dipotassium salt (NADH) were acquired from Sigma-Aldrich Chemical (Milwaukee, WI, USA). Dextran 150 kDa and dextran 500 kDa were acquired from Pharmacosmos (Hoelbrak, Denmark) and used without any further purification.

All of the chemicals were of analytical or spectroscopic reagent grade.

5.1.5. Oxidation of NADH

The reaction was performed at 25 ºC in imidazole-acetic acid buffer. The buffer contained 30 mM of imidazole, 60 mM of CH_3COOK and 30 mM of $MgCl_2$ and was adjusted to pH=7.5. Each sample contains the same concentration of NADH, $1.17 \cdot 10^{-4}$ M, and different LDH concentrations in a range between $1.06 \cdot 10^{-7}$ and $6.36 \cdot 10^{-7}$ M.

Michaelis-Menten plots were obtained by measuring the initial velocity of the reaction at different pyruvate concentrations, in a range between $6.80 \cdot 10^{-5}$ and $7.50 \cdot 10^{-4}$ M. This process was first done without the addition of a crowding agent.

Samples with dextrans content 100 g $\cdot L^{-1}$ of 150 or 500 kDa dextran. The pyruvate solutions were prepared by weighing the required amount of dextran and dissolving it with the corresponding solution. For the enzyme solutions, they were prepared as the dilute solutions but diluting them to the mark with a buffer solution containing 100 g $\cdot L^{-1}$ of 150 or 500 kDa dextran.

The experiment was performed with a stopped-flow valve system; it introduces 100 µL of the solution with enzyme and NADH and 100 µL of the pyruvate solution, it mixes them in a mixing chamber and, after that, it leads them to the measure semi micro cuvette, with a total reaction volume of 200 µL. We observe the change of absorbance that occurs as NADH, which absorbs at 340 nm[3], is oxidized to NAD^+, which no longer absorbs at 340 nm.

The initial reaction rate, v_0, was obtained by linear fitting the initial data points in the absorbance-time plot. A blank solution containing only buffer or buffer with dextran solution was measured in each case.

For each concentration of enzyme we have measured at least two times (three times when performing on solution conditions) the initial velocity in different days and with different enzyme and pyruvate solutions. Every day the initial velocity for one enzyme concentration was

measured at least three times under the same conditions, and same enzyme with NADH solutions and same pyruvate solution in different concentrations.

The NADH solution was prepared daily since it is photosensitive and is degraded easily. The enzyme with NADH solution was prepared for each data set (that is a Michaelis-Menten curve). For each data set, three replicas of each data point were acquired. We have controlled the enzyme activity by measuring frequently a fixed enzyme concentration with the same NADH and pyruvate concentration and comparing the obtained enzyme activity with previous data. We used different batches of enzyme and NADH.

5.2. DATA TREATMENT

The reaction was followed by the spectrophotometric means using a UV-1603 Shimadzu spectrophotometer.

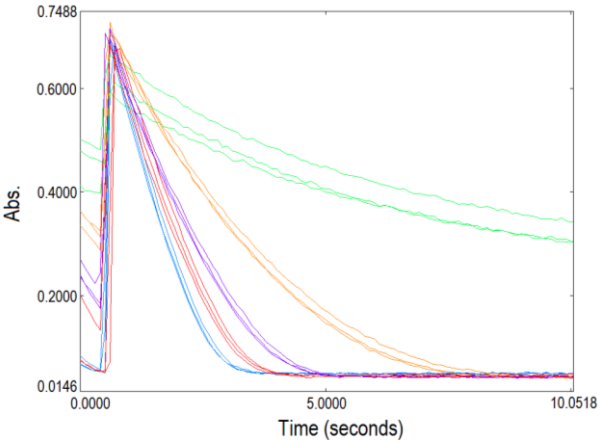

Figure 8. An example of the obtained absorbance curves for a $4.24 \cdot 10^{-4}$ mM enzyme concentration. Pyruvate concentrations: $6.8 \cdot 10^{-5}$ M (green), $2 \cdot 10^{-4}$ M (orange), $3.2 \cdot 10^{-4}$ M (purple), $5 \cdot 10^{-4}$ M (red) and $7.5 \cdot 10^{-4}$ M (blue).

First, we plot the curves in the spectrophotometer data program (UV Probe ver. 2.50), which allow us to see if the curve is valid; an example is presented in Figure 8. That is, the initial linear slope can be clearly seen and there is no noise due to lack of homogeneity (only seen unfrequently in dextran media 100 g/L). Then, if the curves are valid we import them to a data treatment program (Origin ver. 7.0). We plot them again, select the linear section, which is equivalent to the initial rate and is usually between 0.2 and 2 seconds, and perform a linear

fitting of data points. The slope of that line is the initial rate for that pyruvate and enzyme concentrations.

Once we have all the initial rates from different pyruvate solutions on one enzyme concentration for triplicate, we plot them and obtain an average value for each data point. We plot the average value of the initial velocities with its error. We always have obtained Michaelis-Menten curves so we fit the curves to a hyperbolic regression and determine the kinetic parameters. There is an example of a Michaelis-Menten fit in Figure 9, Appendix 1 and the list of Michaelis-Menten fits used in Appendix 2.

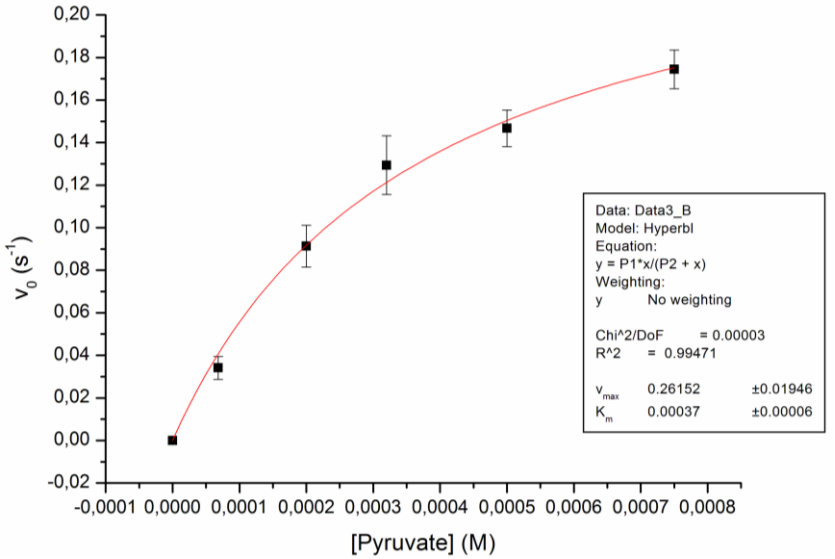

Figure 9. An example of a Michaelis-Menten fitting. Enzyme concentration=$2.12 \cdot 10^{-4}$ mM.

Now we plot the average values of the initial velocities, the substrate concentrations and the enzyme concentration using Gnuplot (ver. 4.6); obtaining a 3D surface plot. We will try to fit our data to a kinetic model in order to obtain the values of the constants that influence our reaction.

As can be seen, the initial velocities are presented, as derivatives in the absorbance, in s^{-1} units. To convert them into $M \cdot s^{-1}$ units, we need to divide them among the molar absorptivity (ε), which has a 6220 $M^{-1}cm^{-1}$ value for the NADH[3], and multiply them by the optical path, which in our case is 1 cm.

6. THEORETICAL BACKGROUND: OLIGOMERIC ENZYME KINETICS

There are many enzymes that are formed by a certain number of subunits or monomers. The subunits are often identical, and each subunit has its catalytic centre. If every site is identical and independent of the rest of sites, the union of a substrate in one catalytic centre will have no effect on the binding properties of the other sites; neither if they are vacant or occupied. This means that an n-site enzyme behaves equal to *n* molecules of a one-site enzyme. [27]

Although there is no obvious interaction between the sites of an enzyme, the isolated monomers are usually found completely inactive. The association to a tetramer may cause changes in the tertiary structure of each monomer, causing changes in the substrate binding. Oligomerization can also contribute to the stability of enzymes in vivo.

If the presence of substrate on one site modifies the substrate binding to the vacant sites or the rate of product formation of the other occupied sites, we have the substrate acting itself as a modifier. These modifications can be substrate activation or substrate inhibition, and are usually known as cooperativity.

Cooperativity is a phenomenon displayed by systems that involve identical o similar molecules that act no-independently of each other. Some enzymes or receptors with multiple binding sites present cooperativity: the affinities for their binding sites vary with the binding of a ligand to a binding site. The word cooperativity arises from “cooperation” between the active sites of polymeric enzymes. [16]

In the enzyme case, we have positive cooperativity when the binding of a substrate molecule helps the binding of another molecule by increasing the affinities of the rest of binding sites. When the binding of a substrate molecule difficult the binding of another molecule by decreasing the affinities of the rest of binding sites we say that the enzyme presents negative cooperativity. [16]

Now we are going to study some cases that are relevant to our reaction and enzyme.

6.1. General case

First, we need to define our enzyme, $E_{s,j}$, s is the number of sites of the enzyme: s=1 monomer, s=2 dimer, s=4 tetramer…; and j is the number of occupied sites independently of their distribution.

Defining the kinetics constants: $k_1^{s,j}$ for the formation of the substrate-enzyme complex, $k_{-1}^{s,j}$ for the dissociation of the complex into the substrate and enzyme and $k_2^{s,j}$ for the formation of the product. The general Michaelis-Menten scheme will be:

$$S + E_{s,j-1} \underset{k_{-1}^{s,j}}{\overset{k_1^{s,j}}{\rightleftharpoons}} E_{s,j} \xrightarrow{k_2^{s,j}} P + E_{s,j-1}$$

Scheme 6. Representation of a Michaelis-Menten enzymatic reaction. The enzyme ($E_{s,j-1}$), with s sites and j-1 occupied sites, reacts with the substrate (S) to form a reversible complex ($E_{s,j}$), with s sites and j occupied sites, that decomposes into the enzyme and the product (P).

Michaelis constants, which are in fact dissociation pseudo-constants of the complexes, will be:

$$K_m^{s,j} = \frac{k_1^{s,j} + k_2^{s,j}}{k_1^{s,j}} \qquad \text{(Eq. 10)}$$

We need to define the intrinsic and the macroscopic or stoichiometric constants. An intrinsic constant is a constant for the site without regard to its association with other sites on the same molecule. It describes the equilibrium between the free substrate, the free site and the site-substrate complex. However, a macroscopic dissociation constant describes the equilibrium between the free substrate, the available enzyme and the enzyme-substrate complex. [27]

When an enzyme contains more than two sites, writing the equilibrium, in terms of macroscopic constants showing each site separately, becomes too difficult. But is relatively easy to write the equilibrium between the various complexes replacing the macroscopic constants by intrinsic constants.

To convert macroscopic constants into intrinsic constants we must consider an entropic term that includes the different distribution ways of the substrate in the free sites. To take into account the distribution of the j occupied sites in the s total sites, is necessary to define the intrinsic constants, which do not depend on the distribution of the occupied sites. To define the

intrinsic constants we need to introduce an entropic term in the equilibrium constant. This term takes into account the relation of distributions between the initial (*j*-1) occupied sites and the *j* sites, when a site will be filled by a substrate.

We can calculate the entropic term as logarithm of the different combinations of occupied sites (*j*-1, j) over *s* total sites:

$$ln\left(\frac{\binom{s}{j}}{\binom{s}{j-1}}\right) = ln\left(\frac{\frac{s!}{j!(s-j)!}}{\frac{s!}{(j-1)!(s-j+1)!}}\right) = ln\left(\frac{s-j+1}{j}\right) \quad \text{(Eq. 11)}$$

From the relationship between equilibrium constant and Gibbs energy ($K^0 = \exp(-\Delta_r G^0/RT) = \exp\{-\Delta_r H^0/RT + \Delta_r S^0/R\}$) and to the fact that in the Michaelis-Menten scheme, $K_m^{s,j}$ is a dissociation pseudo-constant, we are going to use reciprocal constants:

$$K_m^{s,j} = \left(\frac{j}{s-j+1}\right)(K_m^{s,j})^{int} \quad \text{(Eq. 12)}$$

And $k_2^{s,j}$ that is a dissociation of a product, *P,* out of the *j* occupied sites, and there will be *j* possibilities that the dissociation happens:

$$k_2^{s,j} = j(k_2^{s,j})^{int} \quad \text{(Eq. 13)}$$

The velocity equation will be:

$$v = \frac{\mathrm{d}[P]}{\mathrm{d}t} = \sum_{j=1}^{s} j(k_2^{s,j})^{int}\,[E_{s,j}] \quad \text{(Eq. 14)}$$

Applying the stationary state on every intermediate we can obtain a general velocity equation:

$$v = [E_\mathrm{s}]_\mathrm{t}\frac{\sum_{j=1}^{s}\left\{\frac{j(k_2^{s,j})^{int}[S]^j}{\prod_{i=1}^{j}\left(\frac{i}{s-i+1}\right)\left(K_m^{s,i}\right)^{int}}\right\}}{1+\sum_{j=1}^{s}\left\{\frac{[S]^j}{\prod_{i=1}^{j}\left(\frac{i}{s-i+1}\right)\left(K_m^{s,i}\right)^{int}}\right\}} \quad \text{(Eq. 15)}$$

We consider an ideal case when the intrinsic constants are equal:

$$(k_2^{s,j})^{int} \equiv k_2^s \; ; \; \left(K_m^{s,i}\right)^{int} \equiv K_m^s$$

$$v_{max} = s \cdot k_2^s \cdot [E]_t \qquad \text{(Eq. 16)}$$

$$\left(\frac{v}{v_{max}}\right)^{id} = \frac{\frac{1}{s}\sum_{j=1}^{s}\left\{\frac{j\, k_2^s\, [S]^j}{\prod_{i=1}^{j}\left(\frac{i}{s-i+1}\right)K_m^s}\right\}}{1+\sum_{j=1}^{s}\left\{\frac{[S]^j}{\prod_{i=1}^{j}\left(\frac{i}{s-i+1}\right)K_m^s}\right\}} \qquad \text{(Eq. 17)}$$

6.2. Dimer-Tetramer without equilibrium case

Now we are going to study three different cases that are related to our enzyme (LDH): monomer, dimer and tetramer.

The monomer (*s*=1) is always ideal; Its velocity equation is a Michaelis-Menten type of equation and we can define it with one Michaelis constant, K_m^M, and one dissociation constant, k_2^M:

$$\frac{v}{v_{max}^M} = \frac{[S]}{K_m^M + [S]} \qquad \text{(Eq. 18)}$$

where:

$$v_{max}^M = k_2^M \cdot [M]_t \qquad \text{(Eq. 19)}$$

For the ideal dimer case (*s*=2), we have also a Michaelis-Menten type velocity equation. With one Michaelis constant, K_m^D, and one dissociation constant, k_2^D:

$$\left(\frac{v}{v_{max}^D}\right)^{id} = \frac{[S]}{K_m^D + [S]} \qquad \text{(Eq. 20)}$$

where:

$$(v_{max}^D)^{id} = 2 \cdot k_2^D \cdot [D]_t \qquad \text{(Eq. 21)}$$

And if it is not ideal, we will have two Michaelis constants: $K_m^{D_1}$, as a decomposition constant of the *ES₁* complex and $K_m^{D_2}$, for the ES_2 complex; and two dissociation constants: $k_2^{D_1}$, for the *ES₁* complex dissociation and, $k_2^{D_1}$, for the *ES₂* dissociation.

$$\frac{v}{v_{max}^{D_2}} = \frac{\frac{[S]}{K_m^{D_1}}\left(k_2^{int} + \frac{[S]}{K_m^{D_2}}\right)}{1 + \frac{2[S]}{K_m^{D_1}} + \frac{[S]^2}{K_m^{D_1} K_m^{D_2}}} \quad \text{(Eq. 22)}$$

where:

$$k_2^{int} = \frac{k_2^{D_1}}{k_2^{D_2}} \quad \text{(Eq. 23)}$$

$$v_{max}^{D_2} = 2 \cdot k_2^{D_2} \cdot [D]_t \quad \text{(Eq. 24)}$$

For the tetramer case (*s*=4), if it is ideal we will have also a Michaelis-Menten equation with K_m^T and k_2^T, as a Michaelis constant and dissociation constant, respectively:

$$\left(\frac{v}{v_{max}^T}\right)^{id} = \frac{[S]}{K_m^T + [S]} \quad \text{(Eq. 25)}$$

where:

$$(v_{max}^T)^{id} = 4 \cdot k_2^T \cdot [T]_t \quad \text{(Eq. 26)}$$

And if it is not ideal, we will have four Michaelis constants for the decomposition of the four complexes: $K_m^{T_1}$, $K_m^{T_2}$, $K_m^{T_3}$, $K_m^{T_4}$; and four dissociation constants: $k_2^{T_1}$, $k_2^{T_2}$, $k_2^{T_3}$, $k_2^{T_4}$:

$$\frac{v}{v_{max}^{T_4}} = \frac{\frac{[S]}{K_m^{T_1}}\left(k_2^{int,1} + k_2^{int,2}\frac{[S]}{K_m^{T_2}} + k_2^{int,3}\frac{[S]^2}{K_m^{T_2} K_m^{T_3}} + \frac{[S]^3}{K_m^{T_2} K_m^{T_3} K_m^{T_4}}\right)}{1 + \frac{4[S]}{K_m^{T_1}} + \frac{6[S]^2}{K_m^{T_1} K_m^{T_2}} + \frac{4[S]^3}{K_m^{T_1} K_m^{T_2} K_m^{T_3}} + \frac{[S]^4}{K_m^{T_1} K_m^{T_2} K_m^{T_3} K_m^{T_4}}} \quad \text{(Eq. 27)}$$

where:

$$k_2^{int,1} = \frac{k_2^{T_1}}{k_2^{T_4}}; k_2^{int,2} = \frac{k_2^{T_2}}{k_2^{T_4}}; k_2^{int,3} = \frac{k_2^{T_3}}{k_2^{T_4}} \quad \text{(Eq. 28)}$$

$$v_{max}^{T_4} = 4 \cdot k_2^{T_4} \cdot [T]_t \qquad \text{(Eq. 29)}$$

We can conclude that whether the enzyme is ideal or not, v_{max} is always lineal with the total enzyme concentration.

6.3. Dimer-Tetramer equilibrium case

It has been suggested that the LDH enzyme presents a dimer-tetramer equilibrium[26]. We are going to include this condition on the velocity equation deduction and study some cases.

First, we need to define the dimer-tetramer equilibrium:

$$D + D \overset{K}{\rightleftharpoons} T$$

Scheme 7. Representation of the equilibrium between the dimer and the tetramer form of the enzyme.

The first case is the most general and considers an ideal dimer and an ideal tetramer with different values of K_m and k_2. Applying the hypothesis of stationary state and writing the equations in terms of intrinsic constants, we arrive at this expression:

$$v = \frac{2k_2^D}{K_m^D}[S]\left(1 + \frac{[S]}{K_m^D}\right)[D] + \frac{4k_2^T K}{K_m^T}[S]\left(1 + \frac{[S]}{K_m^T}\right)^3 [D]^2 \qquad \text{(Eq. 30)}$$

$$v_{max} = \frac{(k_2^T - k_2^D)}{2K}\left(1 - \sqrt{1 + 8K[D]_T}\right) + 2k_2^T[D]_T \qquad \text{(Eq. 31)}$$

Which gives a non-linear variation on v_{max} with total enzyme concentration.

From balance mass equation for the enzyme:

$$[D] = \frac{\sqrt{\left(1+\frac{[S]}{K_m^D}\right)^4 + 8K[D]_t\left(1+\frac{[S]}{K_m^T}\right)^4} - \left(1+\frac{[S]}{K_m^D}\right)^2}{4K\left(1+\frac{[S]}{K_m^T}\right)^4} \qquad \text{(Eq. 32)}$$

Now we are going to consider a particular case with $K_m^D = K_m^T$ and different k_2. The velocity equation follows a Michaelis-Menten curve with a maximum apparent velocity, v_{max}^{app}, which is non-linear with the total enzyme concentration:

$$v = \frac{v_{max}^{app} \cdot [S]}{K_m + [S]} \qquad \text{(Eq. 33)}$$

$$v_{max}^{app} = \frac{(k_2^T - k_2^D)}{2K} + \frac{(k_2^D - k_2^T)}{2K}\sqrt{1 + 8K[D]_T} + (v_{max}^T)^{id} \quad \text{(Eq. 34)}$$

Finally, if $K_m^D = K_m^T$ and $k_2^D = k_2^T$ then $v_{max}^{app} = v_{max}^{id}$, and the velocity equation follows a n ideal Michaelis-Menten curve:

$$v = \frac{(v_{max}^T)^{id} \cdot [S]}{K_m + [S]} \quad \text{(Eq. 35)}$$

7. ENZYME KINETICS IN DILUTED SOLUTION RESULTS

First, we are going to examine the v_0 ([pyruvate], [enzyme]) function as a surface in a three dimensional plot, in diluted solution conditions. This surface was obtained by plotting all the data points in diluted solution using Gnuplot (ver. 4.6).

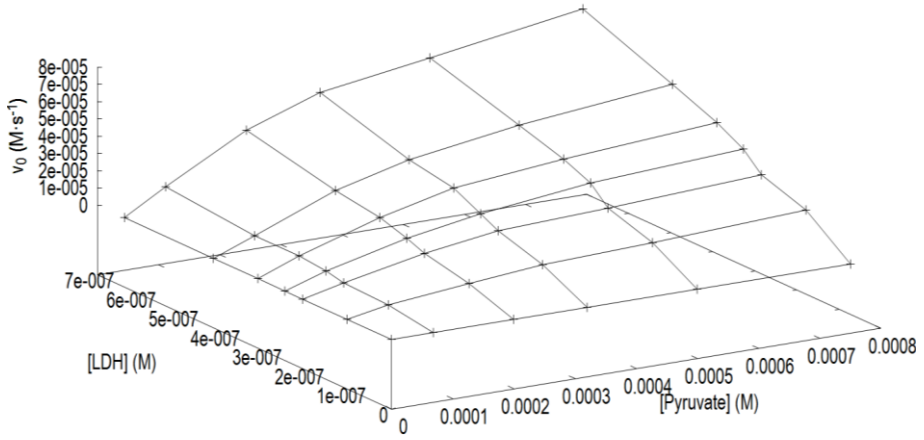

Figure 10. Surface of v_0 ([pyruvate], [enzyme]) of the data obtained working in diluted solution conditions. Note that data is displayed in line-points but no fitting of the data has been performed on this figure.

We have enforced that at [LDH] = 0 and/or [Pyruvate] = 0, the initial velocity is 0.

Now, we are going to examine the surface by plotting the substrate concentration against the initial velocity and the enzyme concentration also against the initial velocity.

First, if we plot the pyruvate concentration against the initial velocity:

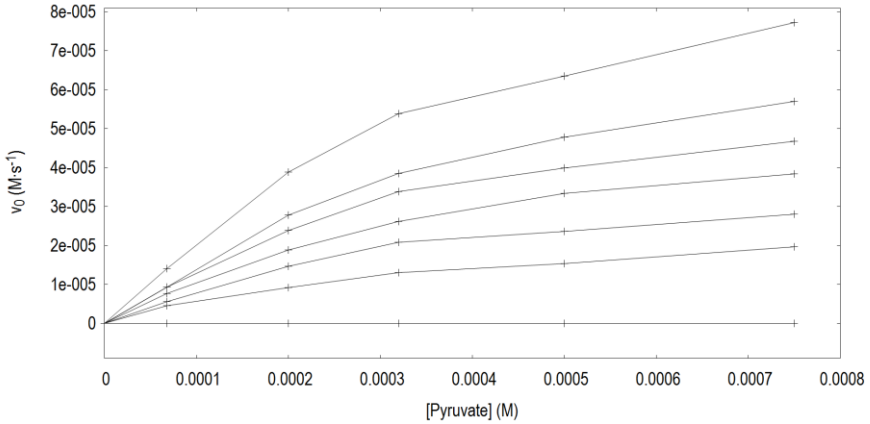

Figure 11. Plot of [Pyruvate] against v_0 of the data obtained working in solution conditions. The different curves are for increasing enzyme concentrations. Note that data is displayed in line-points but no fitting of the data has been performed on this figure.

In Figure 11 we can see that v_0 response against pyruvate concentration is of hyperbolic type for all the enzyme concentrations studied.

The pyruvate concentration in half of the slope (Michaelis constant) of the [Pyruvate] against v_0 curves is practically the same for all the enzyme concentrations. If we examine the K_m values obtained by fitting the curves for different enzyme concentrations in table 1 (all the fittings can be found in Appendix 2), we can see that they are of the same order.

[LDH] (mM)	K_m (mM)
$1.06 \cdot 10^{-4}$	0.47±0.08
$2.12 \cdot 10^{-4}$	0.37±0.06
$2.54 \cdot 10^{-4}$	0.45±0.03
$3.18 \cdot 10^{-4}$	0.39±0.05
$4.24 \cdot 10^{-4}$	0.50±0.06
$6.36 \cdot 10^{-4}$	0.44±0.06

Table 1. Values of K_m at different enzyme concentrations. Average value: 0.44±0.06 mM.

The K_m values obtained are very similar and they do not present any tendency with increasing values of enzyme. The average value for K_m is 0.44±0.06 mM. These results are in agreement with other experimental data reported[8] and with the BRENDA[28] database.

Now, if we examine the dependence of v_{max} with the enzyme concentration:

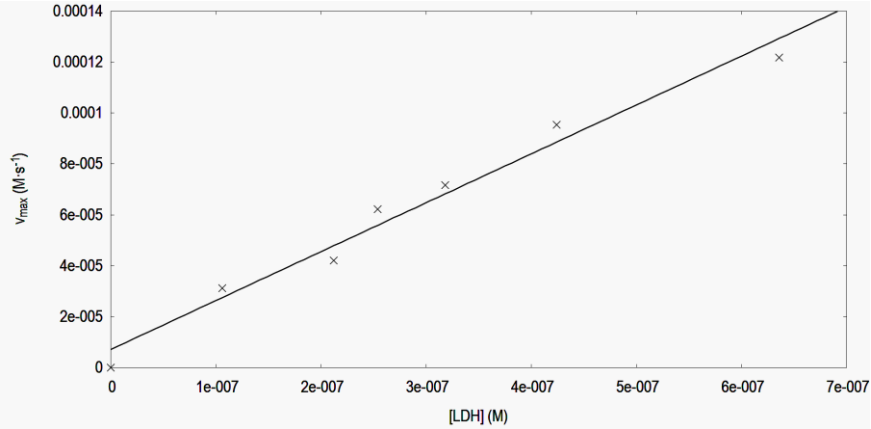

Figure 12. Plot of [LDH] against v_{max} of the data obtained working in solution conditions. The values for v_{max} were obtained from the Michaelis-Menten fittings. The linear fitting was made using Gnuplot: v_{max}=a+b·[LDH] and R=0.98717.

In figure 12 we can see that v_{max} increases with linear tendency with increasing enzyme concentrations. According to *3.1.2.1*, a linear dependence suggests that it is not necessary to take into account the equilibrium between its dimer and tetramer forms. Therefore, we need to fit our data to the cases without dimer-tetramer equilibrium.

First, from the cases without equilibrium, we started with the ideal cases for the monomer, dimer o tetramer. All of them follow a Michaelis-Menten velocity equation; the expression that is needed for the fitting can be easily deduced from the equations in *3.1.2.2*:

$$v = \frac{k_2 \cdot [E]_t \cdot [S]}{K_m + [S]} \qquad \text{(Eq. 36)}$$

Now, fitting all the data represented in Figure 10 to Eq. 36, we have obtained:

Constants		**Error** (%)
$\boldsymbol{K_m}$ (mM)	0.44±0.06	13.7
$\boldsymbol{k_2}$ (s^{-1})	209±14	6.8

Table 2. Constants (K_m, k_2) values obtained by fitting the data in solution media using Gnuplot(ver. 4.6).

As we can see in Table 2, the Michaelis constant value is in agreement with the value obtained averaging the K_m values obtained by fitting individual curves, Table 1. The value is also in agreement to the general K_m values reported in a recent review[29] and with the BRENDA[28] database.

The value of k_2 is in agreement to the general values of catalytic constants reported[29] and to the BRENDA[28] database.

Second, we fitted the non-ideal cases, starting with the non-ideal dimer. The expression used can also be deduced from the equations presented for this case in *3.1.2.2*:

$$v = \frac{\frac{k_2^{D_2}[E]_t[S]}{K_m^{D_1}}\left(\frac{k_2^{D_1}}{k_2^{D_2}}+\frac{[S]}{K_m^{D_2}}\right)}{1+\frac{2[S]}{K_m^{D_1}}+\frac{[S]^2}{K_m^{D_1}K_m^{D_2}}} \qquad \text{(Eq. 37)}$$

The data does not properly fit this equation with assumable errors, and that suggests that our enzyme does not behave like a non-ideal dimer.

Finally, we fitted our data to the expression for a non-ideal tetramer, which can be deduced from the equations described in *3.1.2.2*:

$$v = \frac{\frac{k_2^{T_4}[E]_t[S]}{K_m^{T_1}}\left(\frac{k_2^{T_1}}{k_2^{T_4}}+\frac{k_2^{T_2}}{k_2^{T_4}K_m^{T_2}}[S]+\frac{k_2^{T_3}}{k_2^{T_4}K_m^{T_2}K_m^{T_3}}[S]^2+\frac{1}{K_m^{T_2}K_m^{T_3}K_m^{T_4}}[S]^3\right)}{1+\frac{4[S]}{K_m^{T_1}}+\frac{6[S]^2}{K_m^{T_1}K_m^{T_2}}+\frac{4[S]^3}{K_m^{T_1}K_m^{T_2}K_m^{T_3}}+\frac{[S]^4}{K_m^{T_1}K_m^{T_2}K_m^{T_3}K_m^{T_4}}} \qquad \text{(Eq. 38)}$$

In this case also, the data does not fit properly this equation with assumable errors, and that suggest that our enzyme does not behave like a non-ideal tetramer.

These results reveal that our enzyme seems to not present cooperativity, because the enzyme concentration has a lineal dependence on v_{max}, and our data can be fitted to an ideal model. In conclusion, the results obtained suggest that our enzyme behaves like an ideal non-cooperative tetramer.

8. ENZYME KINETICS IN CROWDED MEDIA RESULTS

We have studied the kinetics in crowded media with two different enzyme concentrations and two sizes of dextran polymer. The aim of this study was to see how crowding can affect our enzyme kinetics. We have chosen two enzyme concentration and performed experiments adding 100 g·L^{-1} dextran concentration using two dextran sizes: 150 kDa and 500 kDa.

We plotted the v_0 against pyruvate concentration curves obtained working in solution and with the two dextran sizes in order to compare the effect of the presence and size of the crowders. The crowding effect will be compared using the variation of the kinetics constants K_m and v_{max}. We are also comparing our results with the one previously obtained[8] in a similar study.

First, for a 2.12·10^{-4} mM enzyme concentration we have obtained:

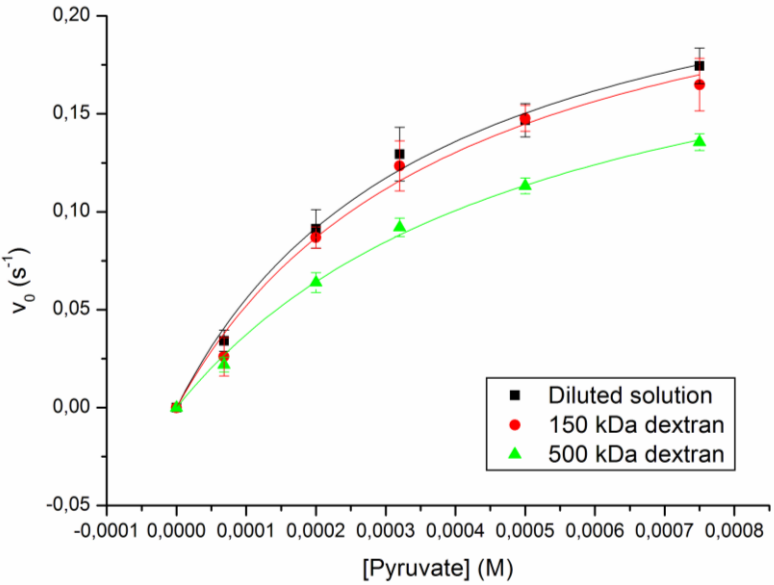

Figure 13. Plot of [pyruvate] against v_0 of the data obtained for a 2.12·10^{-4} mM enzyme concentration working in solution conditions (black squares), with a 150 kDa dextran (red circles) and 500 kDa (green triangles). The dextran concentration for all sizes were 100 g·L^{-1}. The hyperbolic fittings to Michaelis-Menten equation were made using Origin, they can also be found in Appendix 2.

For a $4.24 \cdot 10^{-4}$ mM enzyme concentration:

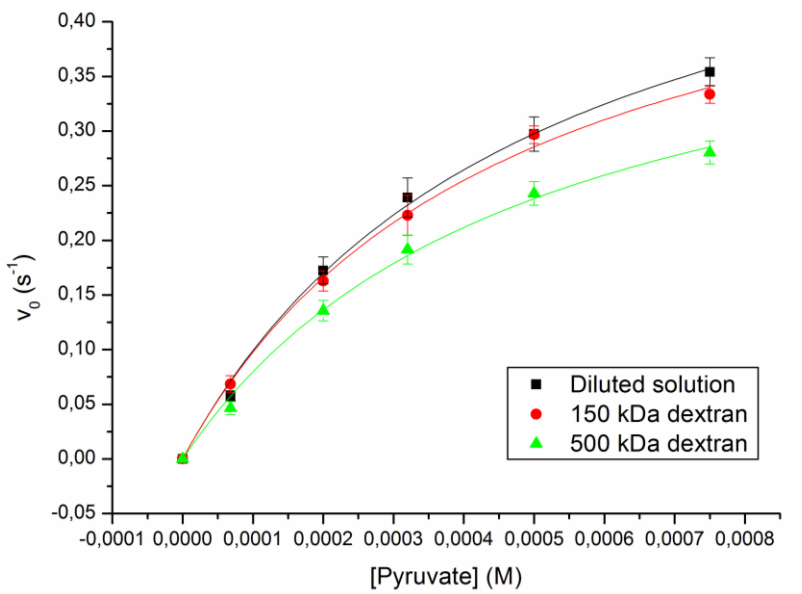

Figure 14. Plot of [pyruvate] against v_0 of the data obtained for a $4.24 \cdot 10^{-4}$ mM enzyme concentration working in solution conditions (black squares), with a 150 kDa dextran (red circles) and 500 kDa (green triangles). The dextran concentration for all sizes were 100 $g \cdot L^{-1}$. The hyperbolic fittings to Michaelis-Menten equation were made using Origin, they can also be found in Appendix 2.

For both enzyme concentrations, 150 kDa dextran does not seem to have an appreciable effect the initial velocity. However, 500 kDa dextran does have a significant effect.

Conditions	**[LDH]** (mM)	v_{max} ($M \cdot s^{-1}$)	K_m (mM)	k_2 ($M \cdot s^{-1}$)
Solution	$2.12 \cdot 10^{-4}$	$(4.2 \pm 0.3) \cdot 10^{-5}$	0.37±0.06	198±14
150 kDa dextran	$2.12 \cdot 10^{-4}$	$(4.2 \pm 0.5) \cdot 10^{-5}$	0.4±0.1	198±24
500 kDa dextran	$2.12 \cdot 10^{-4}$	$(3.7 \pm 0.3) \cdot 10^{-5}$	0.52±0.07	174±14
Solution	$4.24 \cdot 10^{-4}$	$(9.5 \pm 0.5) \cdot 10^{-5}$	0.50±0.06	224±12
150 kDa dextran	$4.24 \cdot 10^{-4}$	$(8.8 \pm 0.6) \cdot 10^{-5}$	0.46±0.05	207±14
500 kDa dextran	$4.24 \cdot 10^{-4}$	$(7.6 \pm 0.5) \cdot 10^{-5}$	0.49±0.07	179±12

Table 3. Values of v_{max}, K_m and k_2 at different enzyme concentrations and in different conditions.

From Table 3, we see that K_m did not significantly change with the presence of any size of dextran and, in average, its value remains practically the same as in the diluted experiments.

Dextran size (kDa)	**[LDH]** (mM)	**Relative decrease in v_{max}**
150	$2.12 \cdot 10^{-4}$	0.0±0.2
500	$2.12 \cdot 10^{-4}$	11.9±0.2
150	$4.24 \cdot 10^{-4}$	7.4±0.4
500	$4.24 \cdot 10^{-4}$	20.0±0.3

Table 4. Values of the decrease in v_{max}, in respect to the solution v_{max} values, for different dextran sizes and enzyme concentrations.

As we can see in Table 3, 150 kDa dextran has not an appreciable effect in $2.12 \cdot 10^{-4}$ mM LDH concentration. However, for an enzyme concentration of $4.24 \cdot 10^{-4}$ mM it has a slightly appreciable diminish effect.

We have obtained similar results with 500 kDa dextran, it has an appreciable effect in both of the enzyme concentrations but it has a higher effect on the most concentrated enzyme concentration, $4.24 \cdot 10^{-4}$ mM.

A hypothesis that could explain this behaviour would be the presence of an auto-crowding effect. Considering a reaction carried out with crowding, with the same substrate concentration and the same crowder concentration: if we increase the enzyme concentration, the velocity of the reaction decreases. It happens because the enzyme itself excludes volume and hinders the diffusion.

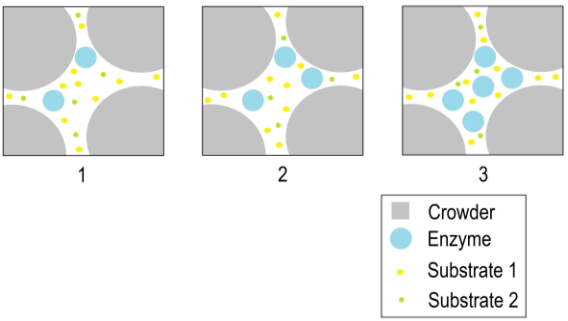

Figure 15. A scheme of the auto-crowding effect. The enzyme concentration increases from left to right images.

If the enzyme concentration increases, the excluded volume increases and the diffusion is hindered, this induces a decrease in the initial velocity. The decrease in the initial velocity causes a decrease in v_{max}.

This hypothesis cannot be guaranteed with only two different enzyme concentrations and two different dextran sizes. To corroborate this effect we would need to repeat our experiments using higher and different enzyme concentrations and different dextran sizes.

Our results are in contrast with the ones reported previously[8]. They obtained that the initial velocity (and v_{max} in consequence) decrease with all the dextran sizes they used, and specifically with the ones that we have used.

This disagreement could be explained by the use of another experimental method. The reported results[8] were obtained by measuring the change in absorbance without a stopped-flow system: by adding the enzyme solution into the measuring cuvette full of pyruvate solution, mixing it manually and measuring. This procedure is not comparable to the stopped-flow method because the mixing of the two solutions is not complete and the enzyme has to diffuse through the solution. In the stopped-flow method, the enzyme and the substrate solutions mix perfectly in the mixing chamber and the dead time in the mixing procedure is within the millisecond scale.

9. CONCLUSIONS

A review on the general enzyme kinetics concepts has been presented and enzyme kinetics models relevant to our case have been discussed. The macromolecular crowding effect and its usual effects on enzyme kinetics have been presented. Some studies related to macromolecular crowding and enzyme kinetics have been reviewed.

A series of experiments spectrophotometrically measuring initial velocity have been conducted varying pyruvate and enzyme concentration. Some experiments have been carried out in solution media and some other experiments have been performed using dextrans with different sizes as a crowding agent.

A surface plot has been obtained for the data working in solution. All the pyruvate against initial velocity curves obtained follow a Michaelis-Menten equation with a similar value for the Michaelis constant. The enzyme concentration against v_{max} plot reveals a linear tendency, suggesting that it is not necessary to take into account dimer-tetramer equilibrium. The data has been fitted to the dimer-tetramer non-equilibrium models proposed and an ideal non-cooperative behaviour has been suggested.

The experiments carried out in crowding media show a higher decrease in the reaction velocity when the bigger dextran and higher enzyme concentration are used. The disagreement with previous experiments has been explained by the change in the methodologies used. An auto-crowding hypothesis is presented but corroboration by performing more experiments is needed.

10. REFERENCES AND NOTES

1. Nelson, D. L., & Cox, M. M. (2008). Lehninger principles of biochemistry. New York City, NY : W.H. Freeman and Co.ISBN 9780716771081
2. Tesch P., Sjödin B., Thorstensson A., Karlsson J. (1978). *Muscle fatigue and its relation to lactate accumulation and LDH activity in man*. Acta Physiol Scand 103 (4): 413–20.
3. Dawson, R. Ben (1985). *Data for biochemical research.* 3rd Ed. Oxford: Clarendon Press. p. 122. ISBN 0-19-855358-7.
4. Van Eerd, J. P. F. M.; Kreutzer, E. K. J. (1996).*Klinische Chemie voor Analisten deel 2.* p. 138–139. ISBN 978-90-313-2003-5.
5. Zimmerman, S. B., and Trach, S. O. (1991) *Estimation of macromolecule concentrations and excluded volume effects for the cytoplasm of Escherichia coli*. J. Mol. Biol. 222, 599−620.
6. Pastor, I., Vilaseca, E., Madurga, S., Garcés, J. L., Cascante, M., & Mas, F. (2010). *Diffusion of alpha-chymotrypsin in solution-crowded media. A fluorescence recovery after photobleaching study*. The Journal of Physical Chemistry. B, 114(11), 4028–4034.
7. Pastor, I., Vilaseca, E., Madurga, S., Garcés, J. L., Cascante, M., & Mas, F. (2011). *Effect of crowding by dextrans on the hydrolysis of N-succinyl-l-phenyl- Ala-p-nitroanilide catalyzed by α-chymotrypsin*. Journal of Physical Chemistry B, 115(5), 1115–1121.
8. Balcells, C., Pastor, I., Vilaseca, E., Madurga, S., Cascante, M., & Mas, F. (2014). *Macromolecular crowding effect upon in vitro enzyme kinetics: mixed activation-diffusion control of the oxidation of NADH by pyruvate catalyzed by lactate dehydrogenase*. The Journal of Physical Chemistry. B, 118(15), 4062–8.
9. Pitulice, L., Pastor, I., Vilaseca, E., Madurga, S., Isvoran, A., Cascante, M., and Mas, F. (2013) *Influence of macromolecular crowding on the oxidation of ABTS by hydrogen peroxide catalyzed by HRP*. J. Biocatal. Biotransform. 2, 1.
10. Homchaudhuri, L., Sarma, N., and Swaminathan, R. (2006) *Effect of crowding by dextrans and Ficolls on the rate of alkaline phosphatase-catalyzed hydrolysis: a size-dependent investigation*. Biopolymers 83, 477−486.
11. Pastor, I., Pitulice, L., Balcells, C., Vilaseca, E., Madurga, S., Isvoran, A., Cascante, M., Mas, F. (2014). *Effect of crowding by Dextrans in enzymatic reactions*. Biophysical Chemistry, 185, 8–13.
12. Poggi, C. G., & Slade, K. M. (2015). *Macromolecular Crowding and the Steady-State Kinetics of Malate Dehydrogenase.* Biochemistry. 2015 Jan 20;54(2):260-7.1115–1121.
13. C. Balcells, I. Pastor, L. Pitulice, C. Hernández, M. Via, J. L.Garcés, S. Madurga, E. Vilaseca, A. Isvoran, M. Cascante and F. Mas. (2015). *Macromolecular Crowding upon in-vivo-Like Enzyme-Kinetics: Effect of Enzyme-Obstacle Size Ratio*. New Front. Chem. 24(1):3-16
14. Ellis RJ (2001). *Macromolecular crowding: obvious but underappreciated*. Trends Biochem. Sci. 26 (10): 597–604.
15. Michaelis, L.; Menten, M.L. (1913). *Die Kinetik der Invertinwirkung*. Biochem Z 49: 333–369
16. Cornish-Bowden, A. (2004) *Fundamentals of Enzyme Kinetics*, 3rd Ed. Portland Press. ISBN 1855781581.
17. Zhou, H.-X., Rivas, G., & Minton, A. P. (2008). *Macromolecular crowding and confinement: biochemical, biophysical, and potential physiological consequences*. Annual Review of Biophysics, 37, 375–397.
18. Hill T. L., *An Introduction to Statistical Thermodynamics*. Dover Publications, New York, 1986,

19. Wang, Y., Sarkar, M., Smith, A. E., Krois, A. S., & Pielak, G. J. (2012). *Macromolecular crowding and protein stability*. Journal of the American Chemical Society, 134(40), 16614–16618.
20. Minton AP. (1989). *Holobiochemistry: an integrated approach to the understanding of biochemical mechanism that emerges from the study of proteins and protein associations in volume-occupied solutions. In Structural and Organizational Aspects of Metabolic Regulation*, Ed. P Srere, ME Jones, C Mathews, pp. 291–306. New York: Liss
21. Vilaseca, E., Isvoran, A., Madurga, S., Pastor, I., Garcés, J.L. and Mas, F., *New insights into diffusion in ·D crowded media by Monte Carlo simulations: effect of size, mobility and spatial Distribution of obstacles.* Phys. Chem. Chem. Phys., 13 (2011) 7396-7407.
22. Pitulice, L., Vilaseca, E., Pastor, I., Madurga, S., Garcés, J. L., Isvoran, A., & Mas, F. (2014). *Monte Carlo simulations of enzymatic reactions in crowded media. Effect of the enzyme-obstacle relative size*. Mathematical Biosciences, 251(1), 72–82.
23. Schöneberg, J., Noé, F. (2013). *ReaDDy – A Software for Particle-Based Reaction-Diffusion Dynamics in Crowded Cellular Environments.* PLOS one, 8(9), e74261.
24. Schnell, S., & Turner, T. E. (2004). *Reaction kinetics in intracellular environments with macromolecular crowding: Simulations and rate laws.* Progress in Biophysics and Molecular Biology, 85(2-3), 235–260.
25. Vilaseca, E., Pastor, I., Isvoran, A., Madurga, S., Garcés, J. L., & Mas, F. (2011). *Diffusion in macromolecular crowded media: Monte Carlo simulation of obstructed diffusion vs. FRAP experiments*. Theoretical Chemistry Accounts, 128(4), 795–805.
26. Saito, M. (1972). *Subunit Cooperativity in the Action of Lactate Dehydrogenase*. Biochim Biophys Acta 258, 17.
27. Segel, I. H. (1993). *Enzyme kinetics: behavior and analysis of rapid equilibrium and steady state enzyme systems.* New York, Wiley.
28. BRENDA: *The Comprehensive Enzyme Information System.* Available in:< http://www.brenda-enzymes.org/>
29. Bar-Even, A., Noor, E., Savir, Y., Liebermeister, W., Davidi, D., Tawfik, D. S., & Milo, R. (2011). *The moderately efficient enzyme: Evolutionary and physicochemical trends shaping enzyme parameters.* Biochemistry, 50(21), 4402–4410.

11. ACRONYMS

LDH: L-lactate dehydrogenase

NADH: Nicotinamide adenine dinucleotide (reduced form)

NAD^+: Nicotinamide adenine dinucleotide (oxidized form)

ALKP: Alkaline phosphatase

MDH: Malate dehydrogenase

HRP: Horseradish peroxidase

FRAP: Fluorescence Recovery After Photobleaching

APPENDICES

APPENDIX 1: EXAMPLE OF THE OBTAINING OF A MICHAELIS-MENTEN FITTING

First, with the initial velocity values obtained from the absorbance curves, for [LDH]= $4.24 \cdot 10^{-4}$ mM in solution:

Day	[Pyruvate] (M)	v_0 (s^{-1})		
16/04/2015	0	0	0	0
	6.80E-05	0.05132	0.05148	0.05803
	2.00E-04	0.15418	0.16029	0.16158
	3.20E-04	0.21193	0.21762	0.221
	5.00E-04	0.27132	0.27789	-
	7.50E-04	0.3442	0.3432	0.33974
17/04/2015	0	0	0	0
	6.80E-05	0.05483	0.05927	0.06433
	2.00E-04	0.17215	0.1919	0.18216
	3.20E-04	0.25703	0.25323	0.24045
	5.00E-04	0.29873	0.31022	0.2966
	7.50E-04	0.35142	0.34865	0.34988
14/05/2015	0	0	0	0
	6.80E-05	0.05943	0.05875	0.06284
	2.00E-04	0.16871	0.17755	0.18299
	3.20E-04	0.2569	0.25366	0.24129
	5.00E-04	0.29813	0.31018	0.31583
	7.50E-04	0.3647	0.36707	0.37808

Table 5. Values of the initial velocity for different pyruvate concentrations and 4.24·10-4 enzyme concentration measured in different days and in solution media.

We need to average the initial velocities:

[Pyruvate] (M)	Average v_0 (s^{-1})
0	0
6.80E-05	0.058±0.005
2.00E-04	0.17±0.01
3.20E-04	0.24±0.02
5.00E-04	0.30±0.02
7.50E-04	0.35±0.01

Table 6. Values of the average initial velocities for different pyruvate concentrations and its corresponding error.

Now, we are going to plot the average initial velocities with its error against the pyruvate concentration and fit them to a hyperbola. The fitting gives us K_m and v_{max}:

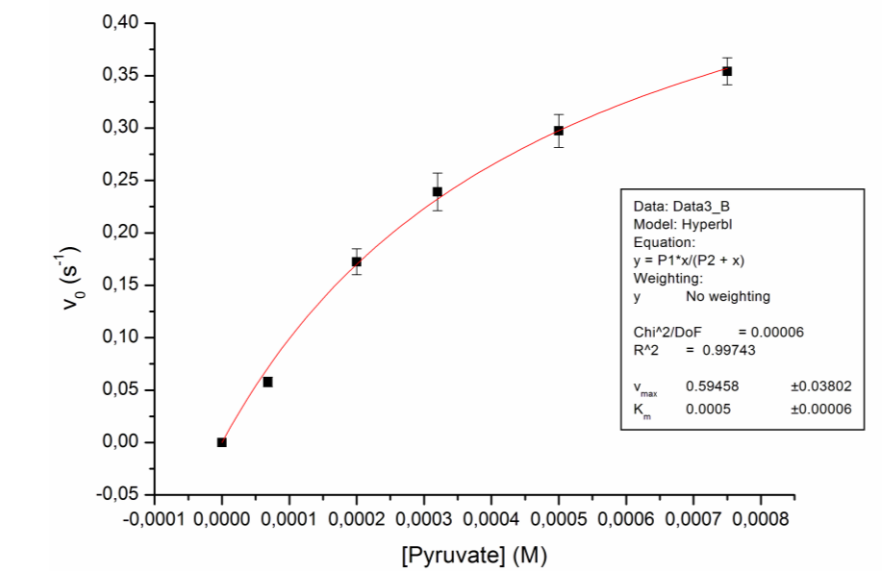

Figure 16. A Michaelis-Menten fitting and plot of the initial velocity against pyruvate concentration for $4.24 \cdot 10^{-4}$ mM enzyme concentration. K_m=0.59±0.04 mM, v_{max}=0.50±0.06 s^{-1}.

A crowded media example is also presented.

Day	**[Pyruvate]** (M)	v_0 (s^{-1})		
19/05/2015	0	0	0	0
	6.80E-05	0.04053	0.04533	0.05466
	2.00E-04	0.13067	0.1243	0.14823
	3.20E-04	0.19307	0.19578	0.21258
	5.00E-04	0.24829	0.24177	0.2554
	7.50E-04	0.27492	0.27742	0.29035
20/05/2015	0	0	0	0
	6.80E-05	0.03425	0.0456	-
	2.00E-04	0.11681	0.14119	0.1338
	3.20E-04	0.18478	0.17226	0.19144
	5.00E-04	0.22372	0.24044	0.2474
	7.50E-04	0.26826	0.29607	0.27476

Table 7. Values of the initial velocity for different pyruvate concentrations and 4.24·10-4 enzyme concentration measured in different days and in crowded media: 500 kDa dextran, 100 g/L.

[Pyruvate] (M)	Average v_0 (s^{-1})
0	0
6.80E-05	0.047±0.006
2.00E-04	0.136±0.009
3.20E-04	0.19±0.01
5.00E-04	0.24±0.01
7.50E-04	0.28±0.01

Table 8. Values of the average initial velocities for different pyruvate concentrations and its corresponding error.

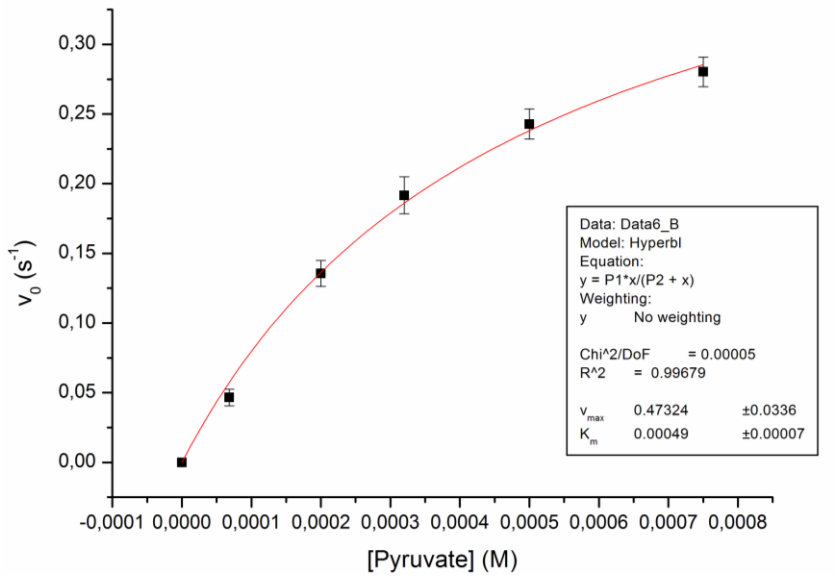

Figure 27. A Michaelis-Menten fitting and plot of the initial velocity against pyruvate concentration for $4.24 \cdot 10^{-4}$ mM enzyme concentration and 500 kDa dextran (100 g $\cdot L^{-1}$). K_m=0.49±0.07 mM, v_{max}=0.47±0.03 s^{-1}.

APPENDIX 2: MICHAELIS-MENTEN FITTINGS

We are going to present the Michaelis-Menten fittings used in this work.

In solution conditions:

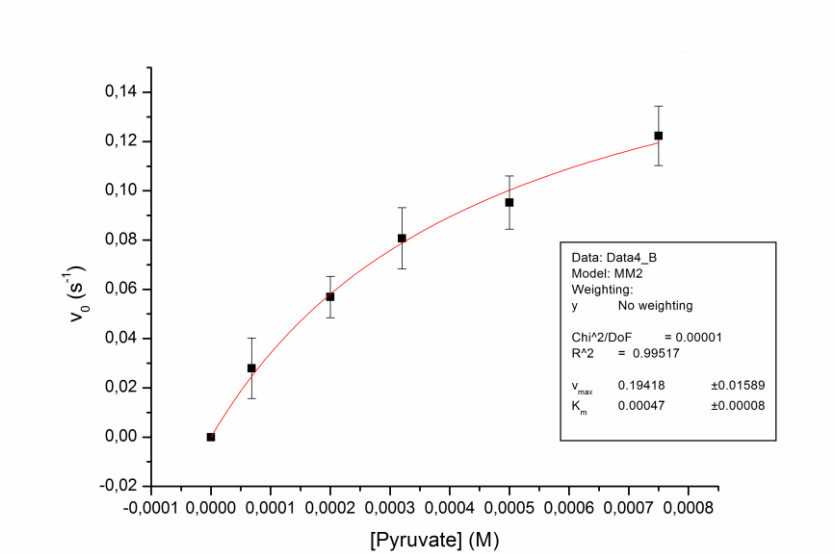

Figure 18. A Michaelis-Menten fitting and plot of the initial velocity against pyruvate concentration for $1.06 \cdot 10^{-4}$ mM enzyme concentration. K_m=0.57±0.08 mM, v_{max}=0.19±0.02 s^{-1}.

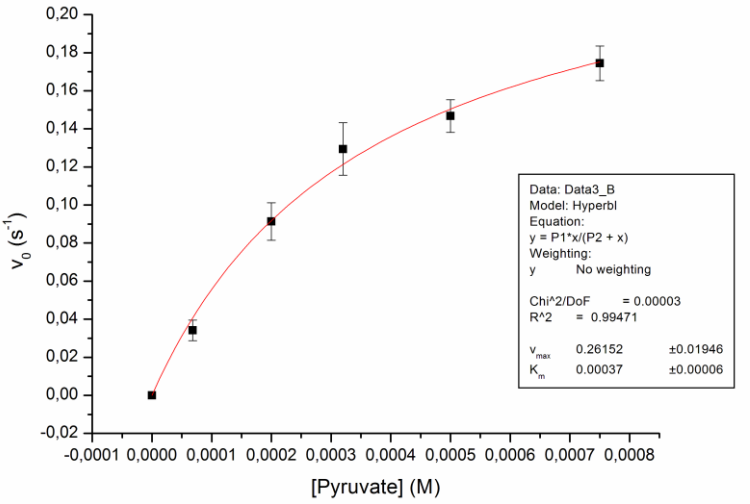

Figure 19. A Michaelis-Menten fitting and plot of the initial velocity against pyruvate concentration for $2.12 \cdot 10^{-4}$ mM enzyme concentration. K_m=0.37±0.06 mM, v_{max}=0.26±0.02 s^{-1}.

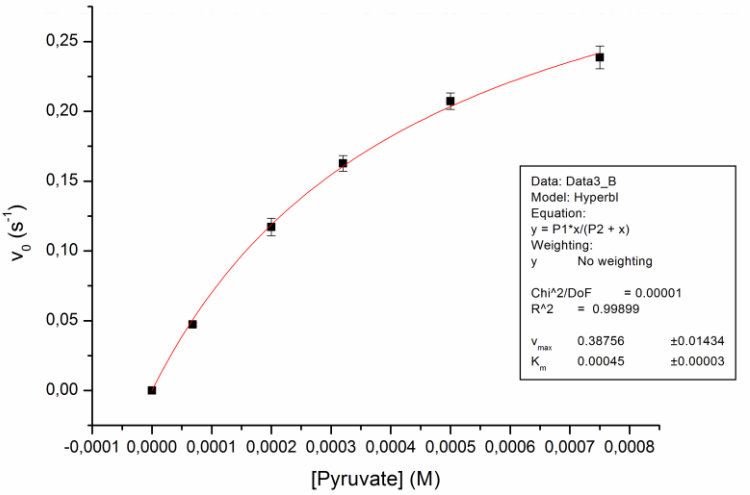

Figure 20. A Michaelis-Menten fitting and plot of the initial velocity against pyruvate concentration for $2.54 \cdot 10^{-4}$ mM enzyme concentration. K_m=0.45±0.03 mM, v_{max}=0.39±0.01 s^{-1}.

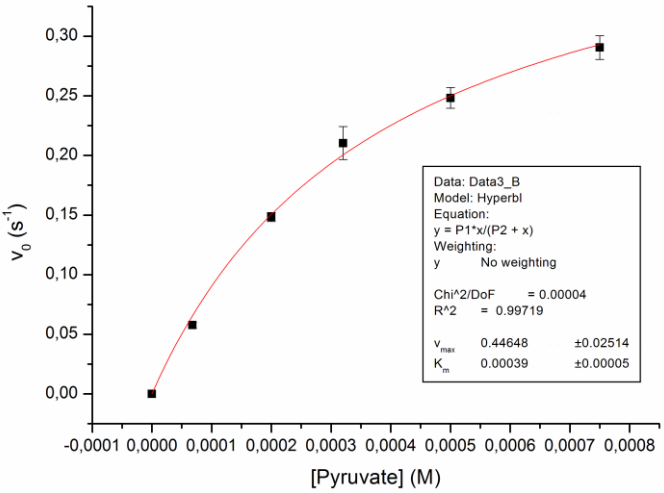

Figure 21. A Michaelis-Menten fitting and plot of the initial velocity against pyruvate concentration for $3.18 \cdot 10^{-4}$ mM enzyme concentration. K_m=0.45±0.013 mM, v_{max}=0.39±0.05 s^{-1}.

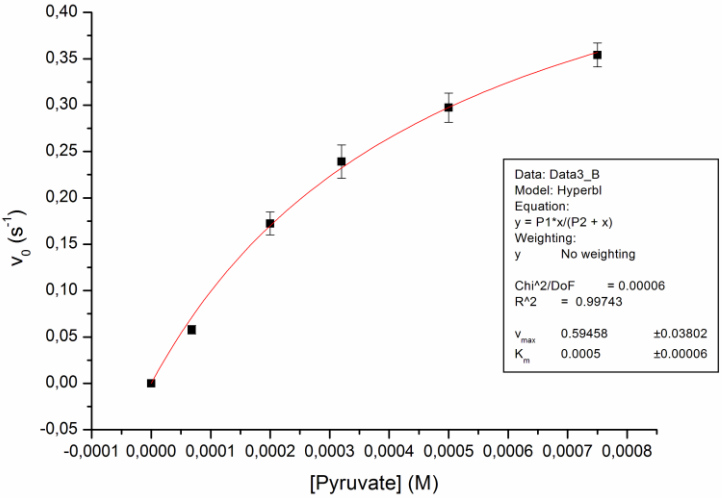

Figure 22. A Michaelis-Menten fitting and plot of the initial velocity against pyruvate concentration for $4.24 \cdot 10^{-4}$ mM enzyme concentration. K_m=0.50±0.06 mM, v_{max}=0.59±0.04 s^{-1}.

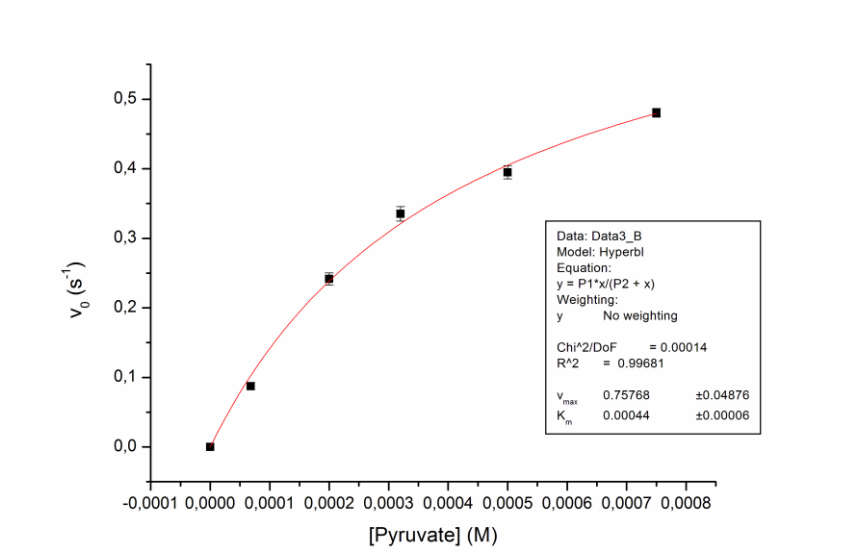

Figure 23. A Michaelis-Menten fitting and plot of the initial velocity against pyruvate concentration for $6.36 \cdot 10^{-4}$ mM enzyme concentration. K_m=0.44±0.06 mM, v_{max}=0.76±0.05 s^{-1}.

Under crowding conditions:

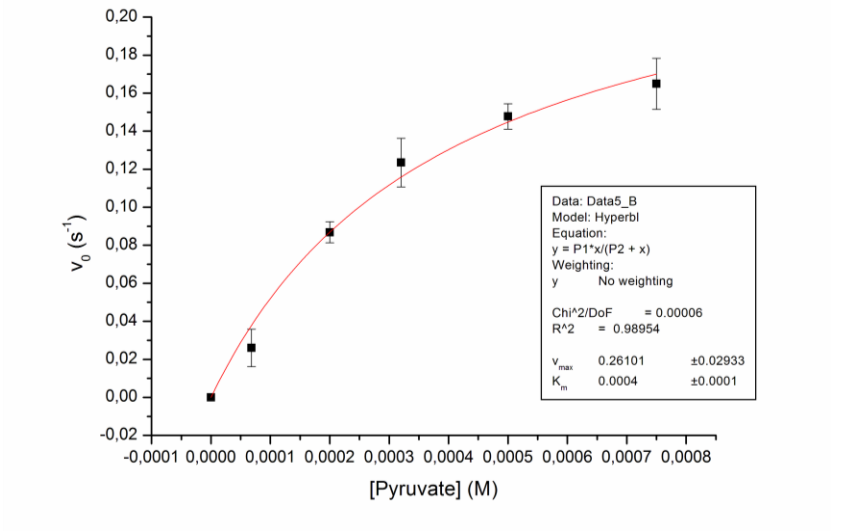

Figure 24. A Michaelis-Menten fitting and plot of the initial velocity against pyruvate concentration for $2.12 \cdot 10^{-4}$ mM enzyme concentration and 150 kDa dextran (100 g $\cdot L^{-1}$). K_m=0.4±0.1 mM, v_{max}=0.26±0.03 s^{-1}.

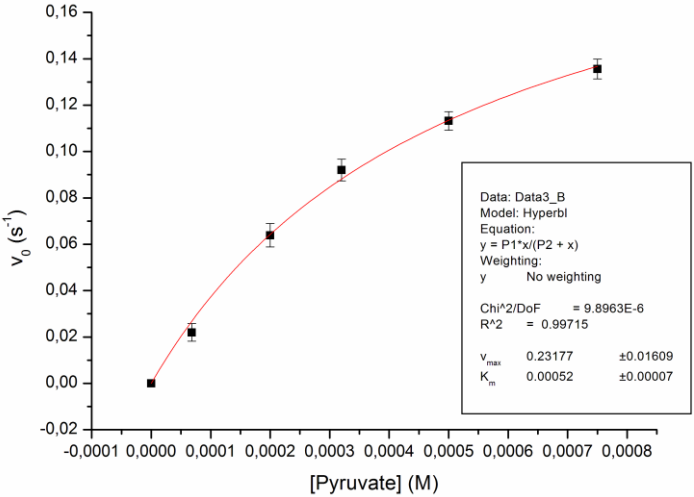

Figure 25. A Michaelis-Menten fitting and plot of the initial velocity against pyruvate concentration for $2.12 \cdot 10^{-4}$ mM enzyme concentration and 500 kDa dextran (100 g $\cdot L^{-1}$). K_m=0.52±0.07 mM, v_{max}=0.23±0.02 s^{-1}.

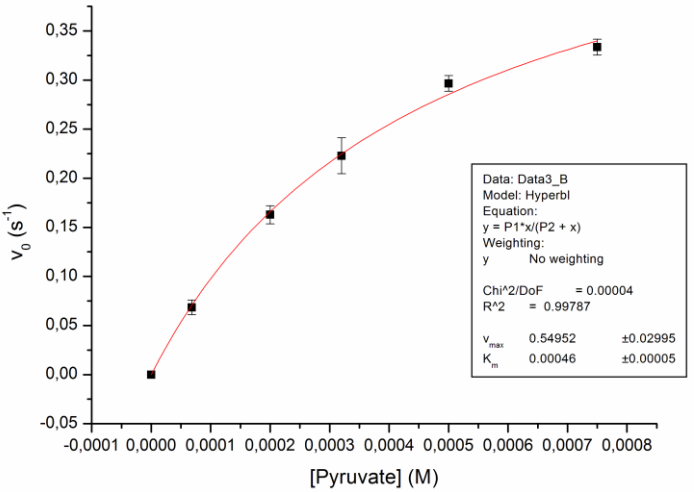

Figure 26. A Michaelis-Menten fitting and plot of the initial velocity against pyruvate concentration for $4.24 \cdot 10^{-4}$ mM enzyme concentration and 150 kDa dextran(100 g $\cdot L^{-1}$). K_m=0.46±0.05 mM, v_{max}=0.55±0.03 s^{-1}.

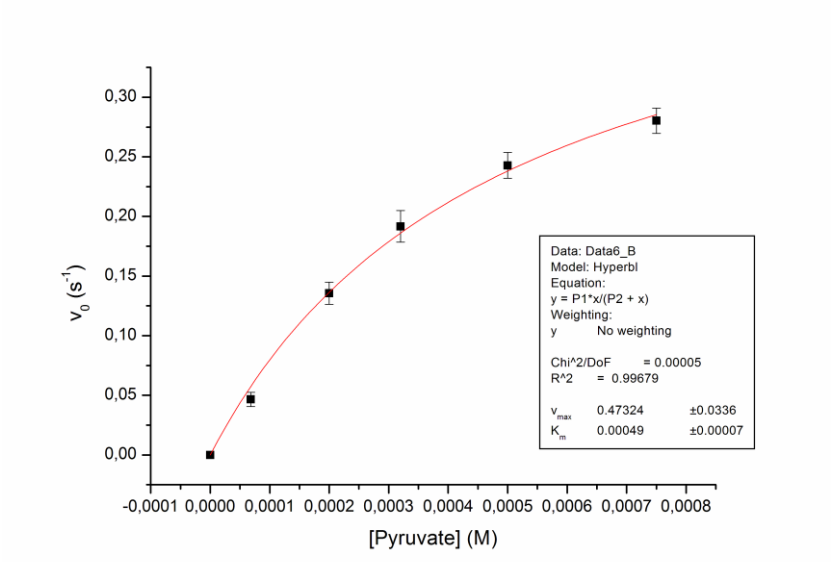

Figure 27. A Michaelis-Menten fitting and plot of the initial velocity against pyruvate concentration for $4.24 \cdot 10^{-4}$ mM enzyme concentration and 500 kDa dextran (100 g $\cdot L^{-1}$). K_m=0.49±0.07 mM, v_{max}=0.47±0.03 s^{-1}.